# Ions and nanoparticles of Ag and/or Cd metals in a model aquatic microcosm: Effects on the abundance, diversity and functionality of the sediment bacteriome

Ana M. Herruzo-Ruiz [a,1], Chiara Trombini [b,1], Ignacio Moreno-Garrido [b], Julián Blasco [b], José Alhama [a], Carmen Michán [a,*]

[a] *Departamento de Bioquímica y Biología Molecular, Campus de Excelencia Internacional Agroalimentario CeiA3, Universidad de Córdoba, Campus de Rabanales, Edificio Severo Ochoa, E-14071 Córdoba, Spain*
[b] *Dpt. Ecology and Coastal Management, ICMAN-CSIC, Campus Rio San Pedro, E-11510 Puerto Real (Cadiz), Spain*

## ARTICLE INFO

## ABSTRACT

Metals can be adsorbed on particulate matter, settle in sediments and cause alterations in aquatic environments. This study assesses the effect of Ag and/or Cd, both in ionic and nanoparticle (NP) forms, on the microbiome of sediments. For that purpose, aquatic controlled-microcosm experiments were exposed to an environmentally relevant and at tenfold higher doses of each form of the metals. Changes in the bacteriome were inferred by 16S rDNA sequencing. Ionic Ag caused a significant decrease of several bacterial families, whereas the effect was opposite when mixed with Cd, *e.g.*, Desulfuromonadaceae family; in both cases, the bacteriome functionalities were greatly affected, particularly the nitrogen and sulfur metabolism. Compared to ionic forms, metallic NPs produced hardly any change in the abundance of microbial families, although the α-biodiversity of the bacteriome was reduced, and the functionality altered, when exposed to the NPs' mixture. Our goal is to understand how metals, in different forms and combinations, released into the environment may endanger the health of aquatic ecosystems. This work may help to understand how aquatic metal pollution alters the structure and functionality of the microbiome and biogeochemical cycles, and how these changes can be addressed.

## 1. Introduction

Aquatic environments are constantly threatened by pollutants as they are heavily influenced by industrial and populated areas. Among the different kinds of pollutants, metals are considered one of the main dangers to these ecosystems as they are widespread, persistent, and potentially toxic, and their rates of mobilization and transport in the environment have increased significantly in the last century (Ali et al., 2019; Tang et al., 2014). Although these pollutants may have a natural origin, *e.g.*, volcanoes, thermal springs, *etc.*, their main sources are related to anthropogenic activities, *e.g.*, combustion vehicles, industrial plants, *etc.* (Algül and Beyhan, 2020; Sall et al., 2020). In any case, directly or indirectly, they are released into aquatic environments continuously, but they are poorly soluble in water. Thus, they can be adsorbed by the sediments and suspended particles, acting as a reservoir for these pollutants, which may degrade the quality of such environments for long periods (Algül and Beyhan, 2020).

Cadmium (Cd) is a toxic metal that accumulates in living organisms producing a wide range of harmful effects and that has also been classified as a human carcinogen. Cd contamination has been widely reported in worldwide sediment samples and water bodies due to its long lasting-nature, tendency to accumulate in organisms, and possible harmful impacts on aquatic ecosystems (recently *e.g.*, (Celis-Hernández et al., 2022; Tian et al., 2022)). Furthermore, bioaccumulation and trophic transfer have also been reported in fish and shellfish, which may lead to some negative consequences such as elevated mortality or reproductive impairment (Bejaoui et al., 2020; Zhang and Reynolds, 2019). The ionic form of silver (Ag) is also well known for its toxicity as it is more harmful to aquatic organisms than any other metal except mercury, although its levels are generally low in contaminated waters (Ndungu, 2011).

The increasing use of nanotechnology has raised questions and

---

concerns about the toxicity of nanoparticles (NPs), including metallic nanoparticles. These materials can act through mechanisms and reactions that are very different from those of their metallic ionic forms and the data available are limited (Oh et al., 2016; Rzigalinski and Strobl, 2009). Cd containing nanoparticles (*e.g.*, CdTeNPs) are used in a wide range of industrial and biomedical applications, such as medical devices, targeted gene and drug delivery, solar panels, display screens, and solid-state lighting as well as exhibiting antibacterial and antifungal biological properties (Solanki and Rajaram, 2017). On the other hand, silver NPs (AgNPs) are some of the most used nanometals in products for human consumption due to their antimicrobial properties, although they can also be toxic to other organisms such as invertebrates, algae or plants (Tao et al., 2016; Yuan et al., 2018).

Although the analysis of nanoparticles in complex environmental matrices is challenging, some information on their concentration in sediment and seawater is available. For example, for AgNPs, Giese et al. (2018) predicted concentrations in the range of 0.02–33.67 µg Kg$^{-1}$ for freshwater sediment and Metcalfe et al. (2018) measured in the range of 1.94–10.18 µg Kg$^{-1}$. In seawater, the concentration was in the range of ng L$^{-1}$ (Wimmer et al., 2020). For CdTeNPs, the concentrations in the aquatic environment are in the range of ng L$^{-1}$. However, to the best of our knowledge, there are no reference values for natural sediments. Nevertheless, the ecotoxicological studies for the assessment of AgNPs and CdTeNPs are in most cases in the range of µg L$^{-1}$ or even higher.

Living beings are not usually exposed to individual pollutants but to a mixture of substances. The combined effect of contaminants, even if at concentrations lower than those that individually produce toxicity, can generate additive, synergistic or even antagonistic effects. Knowledge about the effect of mixtures of metal ionic forms is very limited and practically non-existent if they are in the form of nanoparticles.

Microbial communities form complex and highly connected networks that share and compete for metabolites, and sustain key services of aquatic ecosystems, *e.g.*, pollutant transformation or element cycling. The abundance and diversity of organisms within a certain bacterial community can vary across different temporal scales and in response to biological, chemical or physical stimuli. Therefore, they are particularly sensitive to anthropogenic pressures such as pollution (Wang et al., 2021). While knowledge about the responses of microbial communities to pollution has long been limited, this has changed in recent years due to the implementation of next-generation sequencing. Metagenomic identification of microbes can provide very useful insights not only concerning the structure and phylogenetic biodiversity of the community but also into its metabolic/functional potential (Hu et al., 2021; Wang and Bao, 2022; Yang et al., 2022).

Similarly, understanding the toxicity of a chemical or a chemical mixture regarding a whole ecosystem is much more complex, as not only the physicochemical variables that affect the availability of the chemical/s must be considered but also the interactions between the various compounds and those between the different organisms that are part of the system. An approximation to tackle this complexity is using multispecies/microcosm trials that resemble the environmental conditions in wild ecosystems better.

A multispecies aquatic experimental set-up was designed to analyze the effect of the exposure to Ag and Cd metals, both in their ionic and nanoparticle forms, on the microbiota of aquatic sediments. The selection of these metals and nanoparticles containing them was considering their occurrence in the environment and their toxicity such as antimicrobial properties which make them very relevant to know their impact of environmental microbiome. By doing so, we addressed: (i) the effects of the two forms of Cd and Ag in two different concentrations, one close to environmental levels (Kennish, 2000) and another 10-fold higher, (ii) the consequences of mixing the two metals in each of their forms, and (iii) the differences between exposure to each of the metals, or to the mixture of both, in their ionic form or in the form of NPs. The structure of the sediment's bacterial communities, their diversity and richness, and their potential functionality were determined using high-throughput 16S rDNA sequencing. Our final goals are to improve the knowledge about the impact of pollutants in bacteriome structure and function and the risk assessment of polluted aquatic environments.

## 2. Materials and methods

### 2.1. Design of the artificial aquatic microcosm exposure experiment

A multispecies/microcosm aquatic experiment was designed to evaluate the response of an artificial ecosystem to the presence of metal contaminants, Ag and/or Cd, either in their ionic or nanoparticle forms. Exposure experiments were carried out during 7 days with individual contaminants (Ag, Cd, AgNPs and CdTeNPs) and their binary mixtures (Ag + Cd and AgNPs+CdTeNPs). Both for individual and mixture assays, two different exposure levels were tested: 5 µg L$^{-1}$ close to environmental levels, and a 10-fold higher dose (50 µg L$^{-1}$) (Fig. 1). All the experiments were carried out at the specific facilities in the Institute of Marine Sciences of Andalusia (ICMAN-CSIC) located in Puerto Real (Cadiz, Spain). Fig. 1 shows a scheme of the design. Methacrylate cylinders (120 cm height, 30 cm Ø) filled with a sediment layer (10 cm) and a 19 L seawater column were used. Seawater was collected from the Bay of Cadiz (36°30′0.2,5″ N, 6°15′26.6″ W, Cadiz, SW Iberian Peninsula), decanted for 24 h and 50 µm-filtered to eliminate coarse material in suspension. Natural muddy sediments were collected from the Rio San Pedro intertidal mudflat (36°32′00.1″ N, 6°12′51.9″ W, Cadiz, SW Iberian Peninsula), sieved through a 2-mm nylon mesh to remove large detritus particles and macrofauna, carefully homogenized and stored in darkness at 4 °C until further use. Subsamples of sieved sediment were used for geochemical characterization (humidity, organic matter content, organic carbon content, and percentage of fine particles) and data for each experiment are shown in Supplementary Table S1. Humidity was measured using the weight loss at 100 °C over 24 h. Organic matter content was estimated through calcination (loss of ignition) in a muffle furnace at 450 °C over 24 h. Organic carbon content was determined according to the method described by Gaudette et al. (1974), modified by El-Rayis (1985). The fraction of fine particles was determined by wet sieving with a 63-µm mesh. Model aquatic organisms of different trophic levels were selected for the experiments, two microalgae (*Phaeodactylum tricornutum* and *Nannochloropsis gaditana*) at a density of 10$^4$ cells mL$^{-1}$; *Phaeodactylum tricornutum* is a cosmopolitan species of temperate seas (Bowler et al., 2008) and a standard for toxicity testing by ISO (1995). The *Nannochloropsis gaditana* strain used in this paper (clone B-3, strain CCMM 04/0201) was isolated from the Bay of Cadiz. There are no direct data on the current abundance of either species in the Gulf of Cadiz, but information on the abundance of small phytoplanktonic species in this area (also using *N. gaditana* as a calibration species) can be found in Reul et al. (2006). The crustacean (*Artemia sp.*) is a fairly common organism in the estuaries and salt marshes of the province of Cadiz, although the native species (*Artemia salina*) seems to have been replaced in recent years by an invasive species (*Artemia franciscana*). Abundance data can be found in Amat et al. (2005). Fifty organisms were selected for each experimental cylinder. The bivalve mollusk (*Scrobicularia plana*) is widely distributed in the southwest of the Iberian Peninsula, particularly in the Bay of Cadiz, and lives on muddy sediments. This species has been employed in monitoring activities and ecotoxicity tests (Freitas et al., 2016; Mouneyrac et al., 2014; Solé et al., 2009). Fifteen specimens were employed for each experimental condition. *Artemia* specimens and microalgae were obtained from cultures maintained at the ICMAN-CSIC. Clams (3.15 ± 0.63 cm shell length) were collected from the Rio San Pedro intertidal mudflat (36°32′00.1″ N, 6°12′51.9″ W, Cadiz, SW Iberian Peninsula) and acclimated for 7 days at the ICMAN-CSIC facilities (flow-through seawater system, constant aeration, fed every 48 h with filter feeder's food Tropic Marin Pro-Coral Phyton). The tanks were maintained with aeration, constant temperature and a 12-h light/dark photoperiod. The physico-chemical parameters (pH, temperature, total dissolved solids, conductivity and dissolved oxygen) were monitored
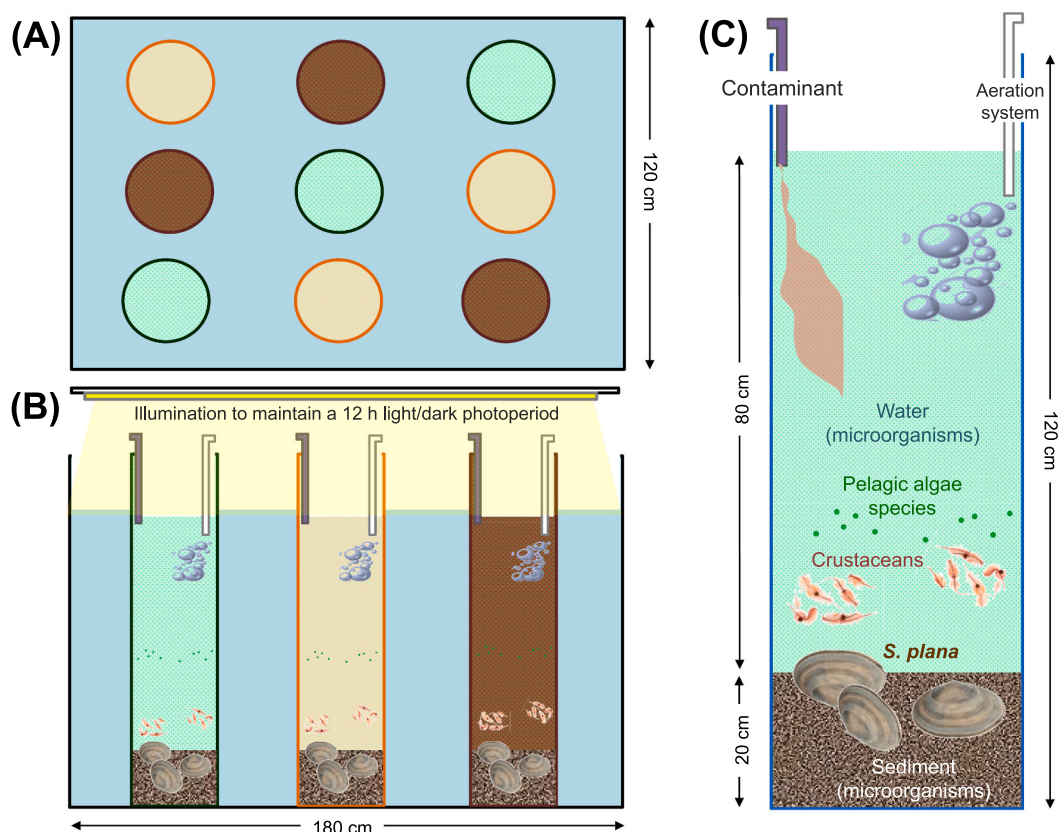
**Fig. 1.** Experimental design of the artificial aquatic microcosms used in the experiments of exposure to pollutants under controlled conditions. A top view (A) and a side view (B) of the tanks used. Each tank contains six individual cylinders, the composition of which is shown in more detail (C): three control cylinders not exposed to pollutant (●), three cylinders exposed to 5 μg L$^{-1}$ (●) and another three cylinders exposed to a 10-fold higher dose (50 μg L$^{-1}$) of the pollutant (●).

throughout the experiment and their average values are reported in Table S2 in the Supplementary Material.

Clams (20 organisms/cylinder) and crustaceans (190 organisms/cylinder) were added at the beginning of the experiment (day 0). Microalgae were added to the microcosms (final density of 10$^5$ cells mL$^{-1}$) every 48 h (days 0, 2, 4 and 6) after being treated as follow: aliquots of both algal species (1 L for *N. gaditana* and 2 L for *P. tricornutum*) were placed in spherical flasks and pre-exposed to the experimental concentration of pollutants for 24 h on an orbital shaker (100 rpm) under continuous white light (around 30 μE m$^{-2}$ s$^{-1}$) and 20 °C (flasks without the pollutants were also set up as controls). After incubation, the cellular density was determined in each flask and appropriate volumes of each culture were centrifuged (Eppendorf model 5810R, at 3000 rpm, 4 °C, 20 min) to concentrate the algae (19·10$^9$ cells in approximately 5 mL) and then they were added to the microcosms. Aliquots (5 mL, 19·10$^9$ cells) of exposed and non-exposed algae were collected to quantify Ag and Cd, centrifuged to remove seawater and stored at −20 °C.

Each exposure experiment was carried out in independent tanks for 7 days before collecting the samples. Six sets of exposure experiments were performed in separate tanks: three for the metallic ions, used individually (Ag, Cd) or mixed (Ag + Cd), and three for their corresponding nanoparticle forms (AgNPs, CdTeNPs and AgNPs+CdTeNPs). Each tank contained 3 control cylinders and 6 cylinders for the exposure to the selected contaminants: 3 exposed to the different contaminants at 5 μg L$^{-1}$, and 3 exposed to a 10-fold higher dose (50 μg L$^{-1}$) (Fig. 1A). The appropriate volumes of 1000 mg L$^{-1}$ stock (1000 mg L$^{-1}$ in HNO$_3$ 0.5 mol L$^{-1}$ for ionic Ag and Cd; 1000 mg L$^{-1}$ in ultrapure water for AgNPs and CdTeNPs; see Section 2.2 for the preparation of the nanoparticles stocks and their characterization), were added on days 0 and 5 to the experimental cylinders to reach the desired nominal concentrations. Stock solutions of AgNPs and CdTeNPs were sonicated (UP 200S Dr. Hielscher GmbH) for 10 min (cycle of 0.5 and frequency of 70 Hz) before the spiking of each system. Water samples were collected on day 0 (before and just after spiking), and on days 1, 5 and 7. On the fifth day, the system was re-spiked and water samples were collected just before and after re-spiking. The samples were stored at −20 °C until metal quantification. Additionally, water samples were collected on days 0 and 7 for nutrient analysis.

At the end of each of the six experiments, samples were collected from the three control replicates and the three tanks exposed to each of the two doses of contaminant. For the current research, sediment samples were then collected in individual Eppendorf tubes and kept at −80 °C until processed. Additionally, aliquots of the sediments were stored (−20 °C) for geochemical characterization (humidity, organic matter, particulate carbon, and percentage of particle <63 μm; the results are shown in Supplementary Table S2), as well as the quantification of Ag and Cd.

### 2.2. Preparation and characterization of Ag and CdNPs

AgNPs (15 nm, US7140) in aqueous suspension were obtained from US Research Nanomaterials. Powder of CdTe Quantum Dots (CdTeNPs; 1.5 nm diameter, emission wavelength at 510 ± 5 nm) was purchased from PlasmaChem GmbH (Berlin) and a 1000 mg L$^{-1}$ stock solution was prepared using ultrapure water.

The particle size for AgNPs and CdTeNPs were analyzed in ultrapure water and marine water by Dynamic Light Scattering (DLS, Zetasizer Nano ZS90, Malvern Instruments, software version 7.10). The agglomeration of AgNPs and CdTeNPs in seawater after 24 h was assessed by DLS (Zetasizer Nano ZS90) showing a change in the average particle size (60 nm and 400 nm, respectively).

## 2.3. Chemical analysis of sediment and water

The ammonium levels in the water samples were quantified according to the Krom method (1980), and expressed as μmol L$^{-1}$.

The Ag and Cd concentrations in the sediment and water were measured by ICP-MS (ICP-MS, Thermo Fisher Scientific™iCAP™ RQ ICP-MS, Waltham, USA). The isotopes used for quantification were $^{107}$Ag and $^{111}$Cd both in sediment and water analyses, and Ag and Cd standard curves were prepared in the same acid matrix used for the samples.

The sediment samples (approximately 0.3 g of freeze-dried sediment) were digested to solubilize the metals using microwave-assisted acid extraction (3 mL HNO$_3$ 65 %, 9 mL HCl 37 %, all Suprapur® quality by Merck, Germany, microwave digester Start D Milestone, according to the procedure described in Application Note HPR-EN-12 from the manufacturing company). Before ICP-MS analysis, the digested samples were made up to 50 mL with ultrapure water, filtered (Glass Fiber, 1 μm) and then 10-fold diluted with ultrapure water to reduce acid content (<2 %). Acid-digested blanks and certified reference material (MESS-3, National Research Council Canada, NRCC) were run with each batch of samples to check the accuracy of the analysis. The recovery with the certified material was 89 % for Ag and 88 % for Cd. The concentrations of Ag and Cd are expressed in μg g$^{-1}$ dry weight (dw). Water samples both from the dissolved and nanoparticle assays, were acidified with HCl (37 %, Suprapur®, Merck, Germany) 0.1 % (v/v) and diluted with ultrapure water by a factor of 20 prior to the ICP-MS analysis. For quality control, blank of the analytical procedure were carried out. Concentrations of Ag and Cd are expressed in μg L$^{-1}$.

The limits of detection (LOD) values were 1.55 ng g$^{-1}$ dw and 0.23 ng g$^{-1}$ dw, respectively, for Ag and Cd in the sediment analyses (for 0.3 g of dry sample), and 0.0012 μg L$^{-1}$ and 0.0027 μg L$^{-1}$, respectively, for the Ag and Cd in the seawater analyses.

Results for the analyses of the ammonium content in the seawater, and the Ag and Cd concentrations in the sediment and seawater are shown in Tables S4-S6.

## 2.4. DNA extraction and bacterial 16S rDNA sequencing

The commercial ZymoBIOMICS DNA Miniprep kit (Zymo Research) was used for the extraction of DNA from the sediments, following the protocol recommended by the manufacturer for soil samples. Two hundred and fifty mg of sediment were used for each extraction. Cell disruption of the microorganisms was carried out in a Disruptor Genie® device (Scientific Industries) at 4 °C for 5 min at maximum speed. Once the cells were lysed, the samples were centrifuged at 10,000$g$ for 1 min and the kit protocol was continued. The genomic DNA extracted was eluted in a final volume of 50 μL. The DNAs isolated were quantified by spectrophotometry and visualized on 1 % agarose gel to check their integrity. Finally, before the 16S rDNA sequencing analysis, samples were tested for amplification using bacterial 16S standard primers to check that they had no PCR inhibitors.

High-throughput sequencing analyses of 16S DNA were performed to identify the different bacterial taxa in the sediments. These analyses were carried out at the Genomic Unit of the Central Service for Research Support (SCAI) of the University of Cordoba (Spain) using the PGM Ion Torrent system, their specific 16S™ Metagenomics Kit (Cat. No. A26216, Pub.no MAN0010799, Thermo Fisher) and the Ion Reporter™ 5.0 software Ion16S Metagenomic analyses module (Thermo Fisher, https://www.thermofisher.com/). Analysis, annotation, and taxonomical assignment were implemented automatically using the mentioned Ion Reporter Software. The length of the amplified fragments varied between 230 and 251 bp, and the number of bases between 28,353,524 and 120,636,049. Those with a quality threshold higher than 20 were selected, and ranged between 25,721,608 and 110,671,146. Finally, the number of reads was between 120,412 and 512,511. The results for V2, V3, V4, V6-7, V8 and V9 primers were analyzed independently, but as V3 always provided the largest and more diverse taxa, they were selected for the taxonomy assignments.

## 2.5. Associations, hierarchical clustering, bacterial alpha-diversity, and functional analyses

MetaboAnalyst5.0 (https://www.metaboanalyst.ca/) was used to perform the statistical analyses to visualize and compute the associations between the different exposures and the variations in taxons. This program offers several options to avoid bias since missing values could alter the analysis, thus impeding data normalization. The default method was selected. This option assumes that half of the minimum positive value for each data set is the detection limit and replaces all the missing and zero values by that number.

Variations in the abundance of the families when exposed to the different contaminants were clustered using the Genesis package. To do so, data were normalized by the Log$_2$ transformation, and the distance measure employed was Pearson's correlation (Sturn et al., 2002).

Bacterial diversity of the sediments was determined calculating their alpha-diversity, to evaluate the richness and uniformity of the microbial populations at the family taxonomic level. The Shannon-Wiener (H') and the Gini-Simpson (D) indices were applied to assess population richness (abundance) (Campo and Duval, 2014), as follows:

$$H' = -\sum \frac{n_i}{N} \times ln\frac{n_i}{N} = -\sum P_i \times lnP_i$$

$$D = 1 - \sum P_i^2$$

where $n_i$ is the number of reads of the $i^{th}$ families; $N$ is the total number of all families in the sample and $P_i = n_i/N$.

Evenness was estimated by the Pielou index (J') (Thukral, 2017) as:

$$J' = \frac{H'}{H'max} = \frac{H'}{lnS}$$

where S is the number of families that have been identified in the study sample and H'max (lnS) the maximum diversity expected.

In addition, a functional data analysis was carried from the metagenomic identifications, using the FAPROTAX software (Python). This software associates the taxonomic categories with previously established metabolic functions or others that are ecologically relevant. For this purpose, FAPROTAX uses a database with the existing literature on the different microorganisms, in such a way that it converts the taxonomic profiles of the microbial community into putative functional profiles (Louca et al., 2016). For this analysis, the cleaned sequences from the 16S DNA sequencing were assigned taxonomy using the SILVA database for bacterial 16S rRNA gene. A single FASTA file format was obtained and used to create an OTU table, which included all the taxonomy information obtained from the sequencing process. Ecologically relevant functions were then assigned to all detected OTUs.

## 2.6. Statistics

The GraphPad Instat (9.0.1, Dotmatics) program was used to analyze the sequencing data statistically. Data were transformed by calculating their binary logarithm (Log$_2$), in order to apply parametric statistical tests subsequently. Since zero values cannot be normalized, before the analysis, any gaps were substituted with the number "9" as the lowest detection limit of the technique is 10 identifications (Vanni et al., 2015). The differences between the means were determined using the two-way ANOVA statistical test, bidirectional analysis of variance, together with the *post hoc* Tukey test with a 95 % confidence interval of analysis. Each of the experiments involving exposure to contaminants was analyzed independently: exposure to Ag, Cd, Ag + Cd, AgNPs, CdTeNPs or Ag + CdTeNPs. The comparisons were: i) Exposure to 5 μg L$^{-1}$ of contaminant *vs.* non-exposed sediments, ii) sediments exposed to 50 μg L$^{-1}$ *vs.*

unexposed ones, and iii) exposure to 50 *vs.* 5 µg L$^{-1}$ of contaminant.

The calculated values for all the diversity parameters were statistically analyzed using a parametric *t*-Student test. The statistical significance of the bacterial identification data and their alpha diversity parameters is represented as: ns (not significant); one symbol, $p < 0.05$; two symbols, $p < 0.01$; three symbols, $p < 0.001$.

## 3. Results

### 3.1. Characterization of aquatic medium and sediment

Low variability was observed in the physico-chemical parameters of the aquatic medium throughout the experiments (Supplementary Table S2). Temperature and pH were in the range of 17.47–21.74 °C and 7.28–8.28, respectively. Dissolved oxygen ranged from 5.19 to 6.52 mg L$^{-1}$. The conductivity and total dissolved content in seawater ranged from 46.58 to 58.76 mS cm$^{-1}$ and from 21.14 to 36.65 g L$^{-1}$, respectively. Data for the Ag and Cd concentrations in seawater for all the assays are presented in Table S6. Metal baseline concentration were in the range of 0.05–0.99 µg L$^{-1}$ and 0.00–9.01 µg L$^{-1}$ for Ag and Cd, respectively. After the spiking, the concentration increased in seawater (1.41–10.77 µg L$^{-1}$ Ag and 2.81–6.37 µg L$^{-1}$ Cd) for the 5 µg L$^{-1}$ nominal concentration, and 18.50–75.99 µg L$^{-1}$ Ag and 29.54–58.42 at 50 µg L$^{-1}$. For NPs, the concentrations detected 30 min after spiking were: 1.32–5.54 µg L$^{-1}$ Ag (exposed to AgNPs) and 1.01–9.87 µg L$^{-1}$ Cd (CdTeNPs) at the 5 µg L$^{-1}$ nominal concentration, and 19.82–62.35 µg L$^{-1}$ Ag (AgNPs) and 12.59–26.79 µg L$^{-1}$ Cd (CdTeNPs) at the 50 µg L$^{-1}$ nominal concentration. The Ag levels in the seawater decreased until reaching a level like the controls or slightly higher depending on the concentration, time and exposure conditions for the ionic and nano-particulate metals. The concentration of Cd in the aqueous phase dropped much more slowly than Ag concentration.

Sediment features presented little variation between the different experiments: values for humidity, organic matter, organic carbon content and fraction of particles <63 µm were 53.42 ± 3.00 %, 8.67 ± 0.73 %, 2.75 ± 0.22 % and 74.12 ± 5.93 %, respectively (Supplementary Table S1).

Results for the quantification of metals in the sediments from all the assays are reported in Table S5. Ag was not detected in the controls (with exception of the Cd assays where Ag at a concentration of 0.067 ± 0.035 µg g$^{-1}$ dw was detected), whereas the concentration of Cd in the controls from all the assays varied between 0.065 and 0.126 µg g$^{-1}$ dw.

Increased concentrations of both metals were recorded in the sediments which were higher at the higher exposure concentrations after 7 days of exposure to the metals. In the assays with metals in ionic forms, the concentration of Ag was 0.146 ± 0.100 µg g$^{-1}$ dw and 0.127 ± 087 µg g$^{-1}$ dw, respectively, in the individual and mixture exposures to 5 µg L$^{-1}$, and 0.496 ± 0.080 µg g$^{-1}$ dw (Ag individual assay) and 0.829 ± 0.196 µg g$^{-1}$ dw (Ag + Cd mixture assay) in the exposure at 50 µg L$^{-1}$. In the sediments from the nanoparticle assays, Ag was only detected at the highest exposure concentration (50 µg L$^{-1}$) (0.176 ± 0.019 and 0.056 ± 0.063 µg g$^{-1}$ dw, respectively, for the individual and mixture assays).

When Cd was present in the system, in ionic form and individually, its concentration in the sediment after 7 days of exposure at 5 µg L$^{-1}$ was very similar to the control (0.105 ± 0.021 *vs.* 0.107 ± 0.019 µg g$^{-1}$ dw); however, the concentration in the systems spiked with 50 µg L$^{-1}$ was approximately 2-fold higher than the control (0.211 ± 0.077 µg g$^{-1}$ dw *vs.* 0.107 ± 0.019 µg g$^{-1}$ dw). The increase of concentration of Cd in the sediment in the spiked systems was more pronounced in the dissolved Ag + Cd mixture assays with a rise of 1.5-fold and 5-fold after exposure to 5 and 50 µg L$^{-1}$, respectively, regarding the control. The Cd concentration in the sediment also increased when this metal was present in the aquatic medium in the NP form, but less than when it was present in the dissolved form. Additionally, increased Cd concentrations were detected at higher spiking levels of the CdTeNPs: 0.099 ± 0.017 µg g$^{-1}$ dw at 5 µg L$^{-1}$ *vs.* 0.134 ± 0.020 µg g$^{-1}$ dw at 50 µg L$^{-1}$.

### 3.2. Global bacteriome analysis

The effects of the exposure to silver, cadmium and their mixture, both in their metallic (Ag, Cd and Ag + Cd) or nanoparticle (AgNPs, CdTeNPs and AgNPs+CdTeNPs) forms, were analyzed in a microcosmic experimental set-up as described in the Material and Methods section. A total of 813,497 identifications were obtained from the 3 exposure conditions (0, 5 and 50 µg L$^{-1}$) and the 3 replicates of the six experiments: 431,188 for the three metallic ion exposures (Ag, Cd and Ag + Cd) and 382,309 for the three exposures to the corresponding nano-particles (AgNPs, CdTeNPs and AgNPs+CdTeNPs) (Table S7). Altogether, the analysis identified 20 phyla. Proteobacteria was the most common phylum accounting for >57.7 % of the identifications, followed by Bacteroidetes (13.0 %), Cyanobacteria (10.5 %), Actinobacteria (7.1 %), Firmicutes (4.7 %), Chloroflexi (2.8 %), Spirochaetes (1.5 %) and Planctomycetes (1.1 %). The rest of the phyla represented <1 % of the total counts. Thirteen phyla were present in each of the six experiments and those not common to all only contributed to 0.04 % of the total counts (Table S7).

Family was the lowest taxonomic level without indeterminations, and thus was selected for further analysis. One hundred and seventy-five families were identified but only 22 were fairly abundant (>1 % of the counts), and all together represented 81.6 % of the total bacteria identified (Table S8). Among these, Ectothiorhodospiraceae, Nostocaceae, Flavobacteriaceae, Desulfobacteraceae and Rhodobacteraceae were the most abundant, ranking from 11.3 to 7.2 % of the identifications. Ninety-three of the most minoritarian families (<0.15 % total identifications) were not present in all six experiments.

### 3.3. Metal modulation of the bacteriome

The number of identifications associated with each phylum and their distribution within each experiment (Ag, Cd, Ag + Cd, AgNPs, CdTeNPs and AgNPs+CdTeNPs) was compared among the three conditions (0, 5, 50 µg L$^{-1}$) (Fig. S1). Roughly, the different exposures did not affect the relative abundance of each phylum under each experimental condition. Proteobacteria was always the most abundant phylum in all the experiments and under all the conditions. Nevertheless, there were slight variations during the experiments, *e.g.*, in the Ag + Cd experiment, Cyanobacteria was the second most abundant phylum followed by Bacteriodetes at the 0 and 5 µg L$^{-1}$ exposures, but this ranking was clearly reversed when exposed to 50 µg L$^{-1}$ of the mixture, or some of the less abundant phyla were only present under certain conditions (Table S7). Nevertheless, none of the changes at this taxonomic level were statistically significant and, thus, this encouraged us to investigate the changes at the family level (Table S8, Table 1).

Statistically significant changes at the bacterial family level upon exposure to the metal ions (Ag and/or Cd), and to the metallic nano-particles (AgNPs and/or CdTeNPs) were analyzed using MetaboAnalyst 5.0 (Table 1, Fig. S2). The identifications at the family level were compared in pairs within each experiment, always comparing a higher concentration with a lower one: 5 *vs.* 0 µg L$^{-1}$, 50 *vs.* 0 µg L$^{-1}$ and 50 *vs.* 5 µg L$^{-1}$ (Table 1). Fifty-one families presented a total of seventy-nine significant changes (Table 1). Most of these changes involved a reduction in the number of counts when the sediments were exposed to increased Ag concentrations (22 decreases *vs.* 3 increases) and an increase when exposed to higher concentrations of Cd or to the Ag + Cd mixture (3 *vs.* 13 or 4 *vs.* 30, respectively). The exposure to nanoparticles produced only four significant alterations: two increments associated to the presence of AgNPs and two reductions when the sediments were exposed to the mixture (AgNPs+CdTeNPs). No significant change was observed for the exposure to CdTeNPs experiment (Table 1).

Significant changes related to the presence of nanoparticles were produced only when the microcosms were exposed to the higher dose and affected only two families: Caldilinaceae that increased moderately (≈4-fold) upon exposure to AgNPs, and Nocardiaceae that decreased

**Table 1**

Statistically significant changes found in sediments at the bacterial family level upon exposure to metals/metallic nanoparticles in a microscosm experimental setup.

| Families | Ag 5 vs. 0 µg L⁻¹ | Ag 50 vs. 0 µg L⁻¹ | Ag 50 vs. 5 µg L⁻¹ | Cd 5 vs. 0 µg L⁻¹ | Cd 50 vs. 0 µg L⁻¹ | Cd 50 vs. 5 µg L⁻¹ | AgCd 5 vs. 0 µg L⁻¹ | AgCd 50 vs. 0 µg L⁻¹ | AgCd 50 vs. 5 µg L⁻¹ | AgNPs 5 vs. 0 µg L⁻¹ | AgNPs 50 vs. 0 µg L⁻¹ | AgNPs 50 vs. 5 µg L⁻¹ | CdTeNPs 5 vs. 0 µg L⁻¹ | CdTeNPs 50 vs. 0 µg L⁻¹ | CdTeNPs 50 vs. 5 µg L⁻¹ | AgNPs+CdTeNPs 5 vs. 0 µg L⁻¹ | AgNPs+CdTeNPs 50 vs. 0 µg L⁻¹ | AgNPs+CdTeNPs 50 vs. 5 µg L⁻¹ |
|---|---|---|---|---|---|---|---|---|---|---|---|---|---|---|---|---|---|---|
| Actinomycetaceae | | | | | | | | | 8.14* | | | | | | | | | |
| Alcanivoraceae | | | | | | 11.27* | | 10.5** | 10.5* | | | | | | | | | |
| Ardenticatenaceae | | | | | | | | | 3.75** | | | | | | | | | |
| Bacillaceae | | 0.45* | 0.44* | | | | | 2.32* | | | | | | | | | | |
| Caldilineaceae | | | | | | | 8.14* | | | | 4.11** | 4.11** | | | | | | |
| Campylobacteraceae | | | | | | | 0.12* | | | | | | | | | | | |
| Candidatus Brocadiaceae | | 0.46** | | | | | | | | | | | | | | | | |
| Cellulomonadaceae | | 0.42* | 0.43* | | | | | | | | | | | | | | | |
| Chitinophagaceae | | | | | | | | 2.27* | 4.88* | | | | | | | | | |
| Clostridiaceae | | | 0.35* | | | | | | | | | | | | | | | |
| Desulfonatronumaceae | | | | | | | | 8.17** | | | | | | | | | | |
| Desulfuromonadaceae | | 0.11** | 0.14* | | | 9.92* | | 7.82* | 28.67*** | | | | | | | | | |
| Erysipelotrichaceae | | 0.25* | | | | | | | | | | | | | | | | |
| Eubacteriaceae | | | | | | | | | 10.00*** | | | | | | | | | |
| Flammeovirgaceae | | | | | | | | 17.33** | 17.33** | | | | | | | | | |
| Geminicoccaceae | | | | | | | | 5.37** | | | | | | | | | | |
| Geobacteraceae | | | | | | | | | 10.09* | | | | | | | | | |
| Halanaerobiaceae | | | | | | | | | 10.83** | | | | | | | | | |
| Hyphomonadaceae | | | | 0.17* | | | | | | | | | | | | | | |
| Lachnospiraceae | 2.19** | | | | | | | | | | | | | | | | | |
| Lentisphaeraceae | | | | | | | | 0.24** | 0.42* | | | | | | | | | |
| Methylococcaceae | | | | | 3.96* | | | | | | | | | | | | | |
| Methylothermaceae | | | | | 6.45* | | | | | | | | | | | | | |
| Microthrixaceae | | | | | 8.27* | | | | | | | | | | | | | |
| Moraxellaceae | | 0.40* | 0.43* | | 3.76* | | | | | | | | | | | | | |
| Natranaerobiaceae | | | | 0.19* | 7.13* | | | | | | | | | | | | | |
| Nitrospiraceae | | | | | 0.15* | | | | | | | | | | | | | |
| Nocardiaceae | | | | | | | | | | | | | | | | | 0.51*** | 0.43* |
| Patulibacteraceae | | 0.11*** | 0.12*** | | | | | | | | | | | | | | | |
| Peptococcaceae | | | | | 93.08*** | | | | | | | | | | | | | |
| Peptostreptococcaceae | | | | | | 6.81* | | | | | | | | | | | | |
| Piscirickettsiaceae | | | | | | | | 2.92* | 4.04* | | | | | | | | | |
| Planctomycetaceae | | | | | | | | 13.33** | 13.33** | | | | | | | | | |
| Polyangiaceae | | 0.19* | | | | | | | | | | | | | | | | |
| Prolixibacteraceae | | | | | | | | 2.73*** | | | | | | | | | | |
| Rhizobiaceae | | | | | | | | 10.50* | 10.50* | | | | | | | | | |
| Rubrobacteraceae | | 0.17* | | | | | | | | | | | | | | | | |
| Saprospiraceae | | 0.08* | | | | | | | | | | | | | | | | |
| Sphingobacteriaceae | | | | | | | | | 7.67*** | | | | | | | | | |
| Sphingomonadaceae | | | | | | | | 7.67*** | 2.63* | | | | | | | | | |
| Spirochaetaceae | | 0.32*** | 0.41* | | | | | | 3.87* | | | | | | | | | |
| Streptomycetaceae | | 0.31* | | | | | | | | | | | | | | | | |
| Syntrophaceae | | | | | | 6.79* | | | | | | | | | | | | |
| Thermoanaerobacteraceae | | | | | | | 0.25* | | | | | | | | | | | |
| Thermoleophilaceae | | | | | | 16.50* | | | | | | | | | | | | |
| unclassified Dehalococcoidia | | 0.20* | 0.15* | | | | | | | | | | | | | | | |
| unclassified Micrococcineae | | | | | 13.00* | 13.00* | | | | | | | | | | | | |
| unclassified Oscillatoriales | | | | | | | | 2.57* | | | | | | | | | | |
| Vibrionaceae | | | | 0.38* | | | | | | | | | | | | | | |
| Victivallaceae | | 8.15* | 8.14* | | | | | | | | | | | | | | | |
| Xanthobacteraceae | | | | | | | | 8.53* | 21.33* | | | | | | | | | |

mildly (≈2-fold) upon exposure to the nanoparticle mixture (AgNPs+CdTeNPs). Significantly, these families were not altered by the presence of the corresponding metallic ions (Table 1).

On the other hand, many bacterial families presented significant changes upon exposure to the metallic forms of Ag and/or Cd (Table 1, Fig. S2). The Ag + Cd mixture experiment showed the highest number (24) of families with significant changes, while 17 and 14 changed in the presence of Ag or Cd, respectively. Furthermore, the extent of the changes also varied widely, from the 93-fold increase in the number of Peptococcaceae identifications when the sediments were exposed to Cd 50 µg L⁻¹, to the 12.5-fold decrease in Saprospiraceae counts when exposed to Ag 5 µg L⁻¹, both compared to their corresponding control. The alterations in the bacterial communities when exposed to the different metal ions were heterogeneous. Only Desulfuromonadaceae was affected by exposure to the single and the combined metals, its presence increased when exposed to Ag, but decreased when exposed to Cd or Ag + Cd combined. The abundance of Moraxellaceae was altered when exposed to the two metals individually but not to the mixture, and again its level was decreased by Ag and increased by Cd. Spirochaetaceae and Bacillaceae were affected by both the Ag and the Ag + Cd exposures showing the same pattern, a reduction in the presence of Ag, and an increase when the mixture Ag + Cd was present. Finally, only Alcanivoracaceae showed significant changes after exposure to Cd and Ag + Cd with similar levels of increase.

When the effects of the two concentrations were individually compared to the unexposed sediments, most of the changes corresponded to the 50 µg L⁻¹ concentration of the metals. The lower levels of the metals only altered 1 family after Ag exposure, 3 for Cd, and 2 for Ag + Cd, while the higher concentration affected 14, 2 and 14, respectively. Also, low and high doses of the metals seem to have opposite effects. With Ag, the exposure to 5 µg L⁻¹ significatively increased the Lachnospiraceae family but the exposure to 50 µg L⁻¹ provoked the decrease of 13 families, with inhibition of up to 9-fold for Desulfuromonadaceae and Patulibacteraceae. Cd and Ag + Cd mixture presented the opposite behavior. Low Cd and Ag + Cd levels decreased the frequency of 3 and 2 families, respectively, being Campylobacteraceae the most affected with an inhibition of >8-fold when exposed to the metal mixture. On the other hand, high Cd and Ag + Cd levels triggered the increase of 2 and 13 families, respectively, with increments of up to 93-fold for Peptococcaceae in the presence of Cd, and 17-fold for Flammeovirgaceae with

Ag + Cd.

Surprisingly, despite the many changes associated with exposure to Ag and/or Cd ions, the microbial diversity for none of the experimental conditions analyzed, measured in terms of richness (Shannon–Wiener's index, *H'*; Gini–Simpson's index, *D*) or evenness (Pielou's method) showed any statistically significant difference (Table S9). On the other hand, although only one family was significantly altered upon exposure to the combination AgNPs+CdTeNPs, the diversity of the bacteriome decreased significantly upon exposure to the higher concentration of the nanoparticle mixture, both in richness (*H'*) and evenness (*J'*) (Fig. 2).

The number of bacterial identifications in the different exposure to metal experiments at the family level was used to perform a PLS-DA analysis with MetaboAnalyst (Fig. 3). The sediments not exposed to metals were separated completely from those exposed to Ag and/or Cd, both in the metallic form (A) and as nanoparticles (B). On the other hand, the sediments exposed to metal concentrations 5 and 50 µg L⁻¹ overlapped in all six experiments. The greatest separation was generally found between the exposure to the 5 µg L⁻¹ concentration and the control that was not exposed to metals.

### 3.4. Trends in the bacteriome in response to the metallic forms of Ag and/or Cd

While there were very few changes when the metals were added in the nanoparticle form, many bacterial families were altered when exposed to the metal ions Ag and/or Cd. Therefore, the relative abundance of the families showing statistically significant differences upon exposure to the metallic forms of Ag, Cd or Ag + Cd were used for a cluster analysis using the Genesis algorithm to see if they followed similar patterns (Fig. 4). The bacterial families from the Ag experiment were separated into three different clusters but most of the taxa (16 out of 17) followed trends I and II, as their abundance clearly decreased upon exposure to the highest concentrations of the metal. On the other hand, families from the Cd and Ag + Cd experiments were divided into only 2 clusters, III and IV, with most of the families presenting their highest levels at the highest concentration (50 µg L⁻¹) used in this work of Cd or of the Ag + Cd mixture. The 21 families that followed trend III after exposure to the highest concentration of the mixture of Ag + Cd should be highlighted because of their number. Of them, only Desulfuromonadaceae (Cluster IV) and Alcanivoracaceae (Cluster III) showed
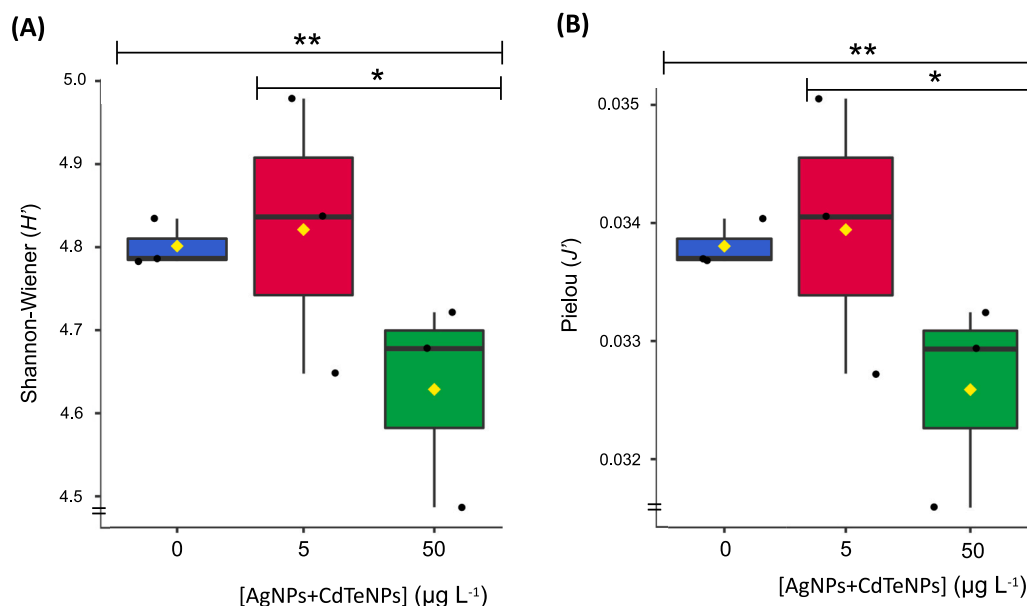
**(A)**



**(B)**



**Fig. 2.** Diversity indices at the family level in sediments when exposed to increasing concentrations of the mixture of the metallic nanoparticles (AgNPs+CdTeNPs). The Shannon-Wiener's (A) and the Pielou's indices (B) were determined as described in the Material and Methods section. Statistically significant differences are indicated as: *, $p < 0.05$; **, $p < 0.01$; ***, $p < 0.001$.

a similar trend when exposed to the highest Cd concentration. In contrast, Desulfuromonadaceae (Cluster I), and Bacillaceae (Cluster II), showed an inverse trend after exposure to the highest Ag concentration.

### 3.5. Functional changes in the bacteriome related to the presence of metals

The influence of the metals on the functional changes of the bacteriome present in the sediments was evaluated by using the FAPROTAX database. The species identified were assigned to 54 functional groups (Table S10). Globally, the function with the highest number of bacterial species assigned was "chemoheterotrophy" with 112 species followed by "aerobic chemoheterotrophy" with 86, and "fermentation" and "nitrate reduction" with 36 species each. "Chemoheterotrophy" and "aerobic chemoheterotrophy" were also the functions with the highest counts associated, 45,222 and 33,610, respectively. On the other hand, functions such as "dark oxidation of sulfur compounds" and similar were inferred from a small number of species (6–9) but had a high number of associated identifications ($\approx$11,000).

To determine whether the presence of the different metals could affect the metabolic capacity of the bacteriome in the sediments analyzed, the abundance of the different species associated to the potential functions by FAPROTAX was evaluated statistically by ANOVA for each of the experiments (Fig. 5). Of all the six experiments, and in agreement with the changes at the family level, only those exposed to Ag, Ag + Cd and AgNPs+CdTeNPs showed significant differences in their bacteriome associated functions when exposed to the different doses of the metals (Fig. 5). The changes after exposure to Cd, AgNPs and CdTeNPs were not statistically relevant. Some functions were merged by integrating those performed by the same microorganisms to simplify Fig. 5. Most of the changes occurred when the sediments were exposed to the highest concentration of the metals (50 μg L$^{-1}$). Further, in agreement with the family abundance profiles (Fig. 4), the metabolic potential associated with exposure to Ag was found to decrease at the highest metal concentration, while the functional changes associated with the presence of Ag + Cd increased greatly at 50 μg L$^{-1}$ (Fig. 5). Thus, the two common categories for both exposures "human associated/pathogens all" and "phototrophy" showed opposite patterns when exposed to only Ag or to the Ag + Cd mixture. Processes related to

"nitrogen and sulfur metabolism" and to the anaerobic "respiration" of different electron acceptors compounds (iron, fumarate, manganese, sulfur and sulfate) were clearly inhibited when the sediments were exposed to Ag, which may affect the biogeochemistry of these anaerobic environments. "Animal parasites and symbionts" were also repressed. On the other hand, "dark oxidation" of different compounds (hydrogen, sulfur, sulfide and thiosulfate) is clearly promoted by the exposure to combined Ag and Cd ions. Although only one family significantly varied when the sediments were exposed to AgNPs+CdTeNPs (Table 1), several potential functions were reduced at the highest dose of the mixture of metallic nanoparticles (Fig. 5). The very significant inhibition of those microorganisms related to the "fermentation" and anaerobic "respiration" of several compounds (fumarate, sulfur, iron and manganese) is to be noted, just as that which occurred after exposure to Ag. Other processes such as "chemoheterotrophy" and "lithic" processes (ureolysis and xylanolysis) were also negatively affected by the highest dose of the NP mixture (Fig. 5).

### 4. Discussion

#### 4.1. Dynamic of distribution of metals in the aquatic environment

The behavior of dissolved metals and nanoparticles in seawater is conditioned by a wide variety of factors such as: the presence of ions (Na$^+$, Mg$^{2+}$, Cl$^-$ and SO$_4^{2-}$), natural organic matter (NOM; fulvic and humic acids) and substances produced by phytoplankton (polysaccharides, amino acids, *etc.*). Free Ag and Cd ions, the most bioavailable and toxic forms for many aquatic organisms, may adsorb onto hetero-particles (NOM, clay or silt) or react with ions (particularly with Cl$^-$ and SO$_4^{2-}$) to form stable compounds (AgCl$_x^{1-x}$, Ag$_2$SO$_4$, CdCl$^+$, CdCl$_2$, *etc.*) that tend to settle in the sediment, thus producing a reduction of the ionic content in seawater and an increase in the concentration of metals in sediments (Celis-Hernández et al., 2022; Chronakis et al., 2023; Zhao et al., 2013). On the other hand, metallic nanoparticles in seawater are subject to various reactions, which is why they can be found in this medium in different forms: homo (NP-NP complexes) and hetero-aggregates (NP-NOM complexes) (with a high tendency to settle in the sediment), free ionic metals (from dissolution processes) and inorganic complexes (reaction with ions present in the seawater)
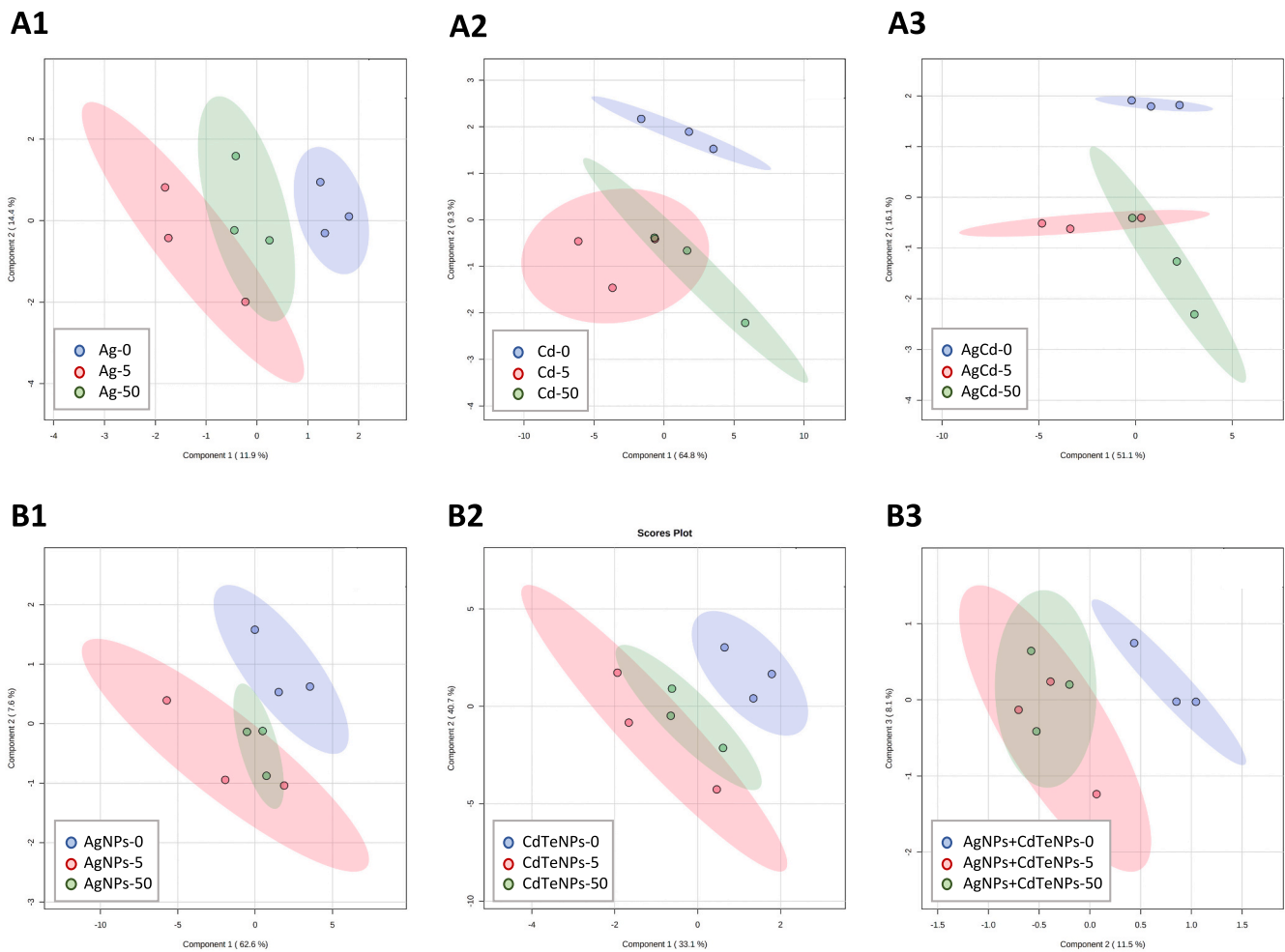
**Fig. 3.** PLS-DA analysis of the bacterial families in the sediments when exposed to Ag (1), Cd (2) or to a mixture of Ag and Cd (3), both in the metallic form (A) and as nanoparticles (B). The three experimental replicates were grouped using the supervised multivariate regression PLS-DA analysis performed with MetaboAnalyst 5.0 software. Sediments not exposed to the metals are represented in blue, while those exposed to 5 μg L$^{-1}$ and 50 μg L$^{-1}$ metal concentrations are shown in red and in green, respectively. (For interpretation of the references to color in this figure legend, the reader is referred to the web version of this article.)

(Chronakis et al., 2023; Li et al., 2020b; Rocha et al., 2015b; Wimmer et al., 2020). The toxicity of the nanoparticles is related both to their particulate and dissolved forms (Graves, 2022). The sedimentation processes that occur for both ionic and nanoparticulate Ag and Cd explain the decrease in the concentrations of both metals in seawater and their accumulation metals in the sediments that was observed in our experiments. Marine sediments act as a sink for metals but also as an important source and exposure route to these contaminants for benthic organisms, particularly microorganisms (Zhao et al., 2021). Through processes such as the decomposition of organic matter and the dissolution of NPs-aggregates, Ag and Cd can be released to the surface of the sediment and sediment pore water where they can interact with bacteria and microorganisms by altering genetic, biochemical and metabolic processes, microbial biomass and community structure (Abu Bakar et al., 2022; Pan et al., 2022).

The simultaneous presence of species from different trophic levels (algae, crustaceans and bivalves) in the microcosm has made it possible to explore more complex relationships. Microalgae are known to accumulate metals in both dissolved and nanoparticulate forms (Sendra et al., 2017). Metals can be adsorbed on the surface of microalgae or internalised (Levy et al., 2008). In both cases, they can contribute to accumulation of metals to higher levels (*e.g.*, crustaceans and bivalves) through predation and trophic transfer (Babaei et al., 2022). *Artemia sp.* can accumulate dissolved metals and metallic nanoparticles (Bhuvaneshwari et al., 2018). Clams take up metals from food and water

(Kalman et al., 2014). At the end of the experiment, a clear accumulation pattern (balance between uptake and excretion) was reported in the two target tissues, the gills and the digestive gland, for single and mixed metals. Nevertheless, the rate of accumulation depends on the metal (Serafim and Bebianno, 2010) and, for nanoparticles, on their composition and their chemical behavior (Rocha et al., 2015a), as in some cases no real accumulation is observed because they can be eliminated in a significant way through faeces or pseudofaeces (Volland et al., 2015).

*4.2. Analysis of the microbiome to monitor the wellbeing of the aquatic environment*

Current estimations predict that there are up to $10^{12}$ species of prokaryotes on Earth that control major biogeochemical cycles and other essential functions (Averill et al., 2022; Locey and Lennon, 2016). Microbial communities are influenced by anthropogenic activities, exemplified by recent extinction and co-extinction processes linked to current environmental changes that are leading to a decrease in global diversity (Averill et al., 2022). Furthermore, changes in the abundance of microorganisms are likely to be better bioindicators for subtle pollution events than macroscopic species as they are more ubiquitous, they are the first to encounter pollutants and they have quick population dynamics. Thus, studying and understanding microbial changes due to pollution is pivotal to prevent and to revert negative micro- and macrobiological effects (Averill et al., 2022).
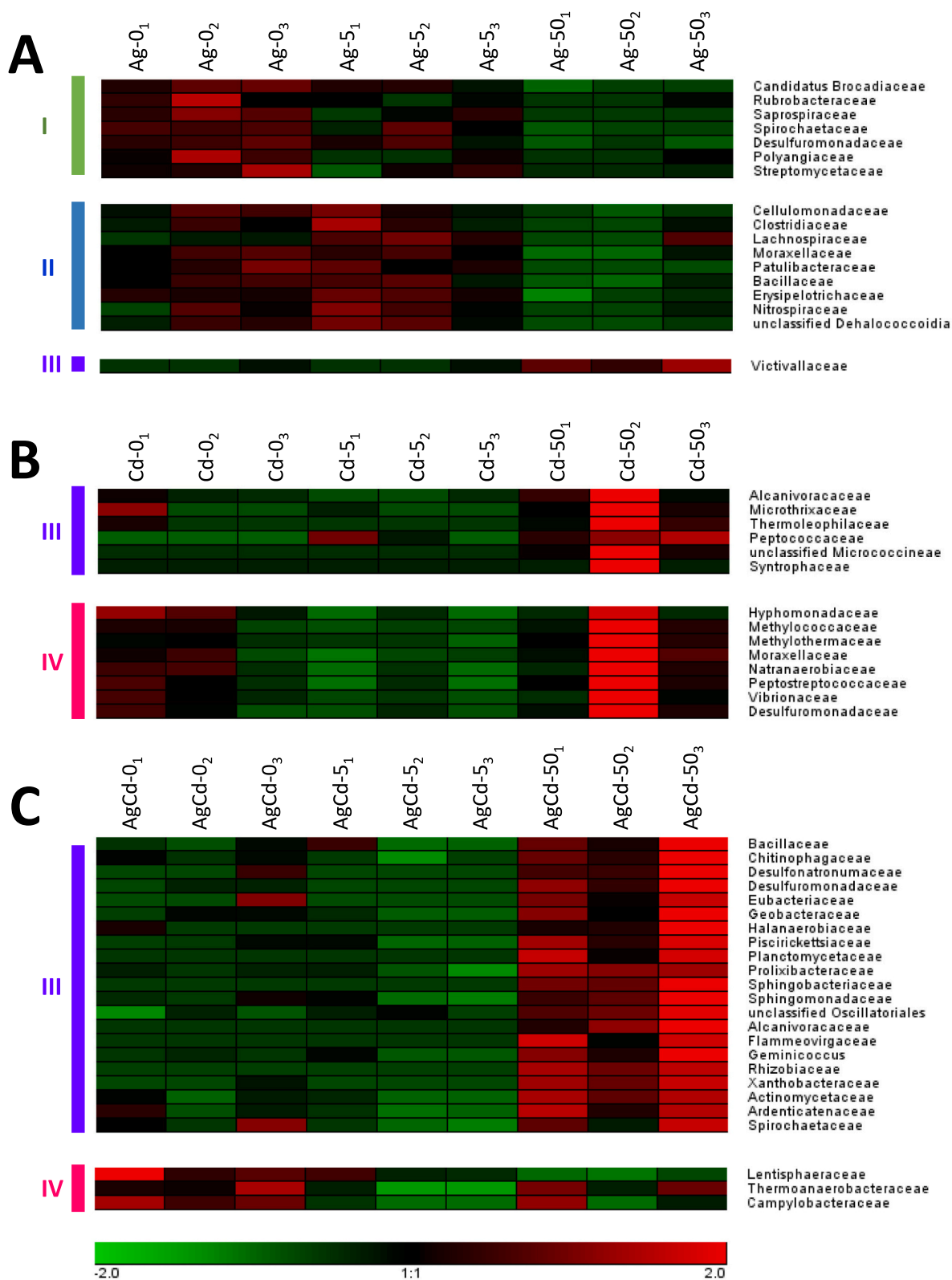
**Fig. 4.** Cluster analysis of the bacterial families showing significant differences in abundance when exposed to the metallic form of Ag and/or Cd. The k-means method, using the Genesis software (Sturn et al., 2002), was used to cluster the families that changed when sediments were exposed to Ag (A), Cd (B) or the Ag + Cd mixture (C). Only families with statistically significant changes were used for the analysis. Relative abundance is represented in a heat map with colors ranging from green to red, which expresses the relative gradation from low to very abundant populations, respectively, in each experiment. The bacterial families are grouped in three clusters for Ag exposure and two clusters for Cd and Ag + Cd exposures. Four different clusters could be grouped in the 3 experiments (labeled with I–IV and different colors on the left hand of the figure). (For interpretation of the references to color in this figure legend, the reader is referred to the web version of this article.)
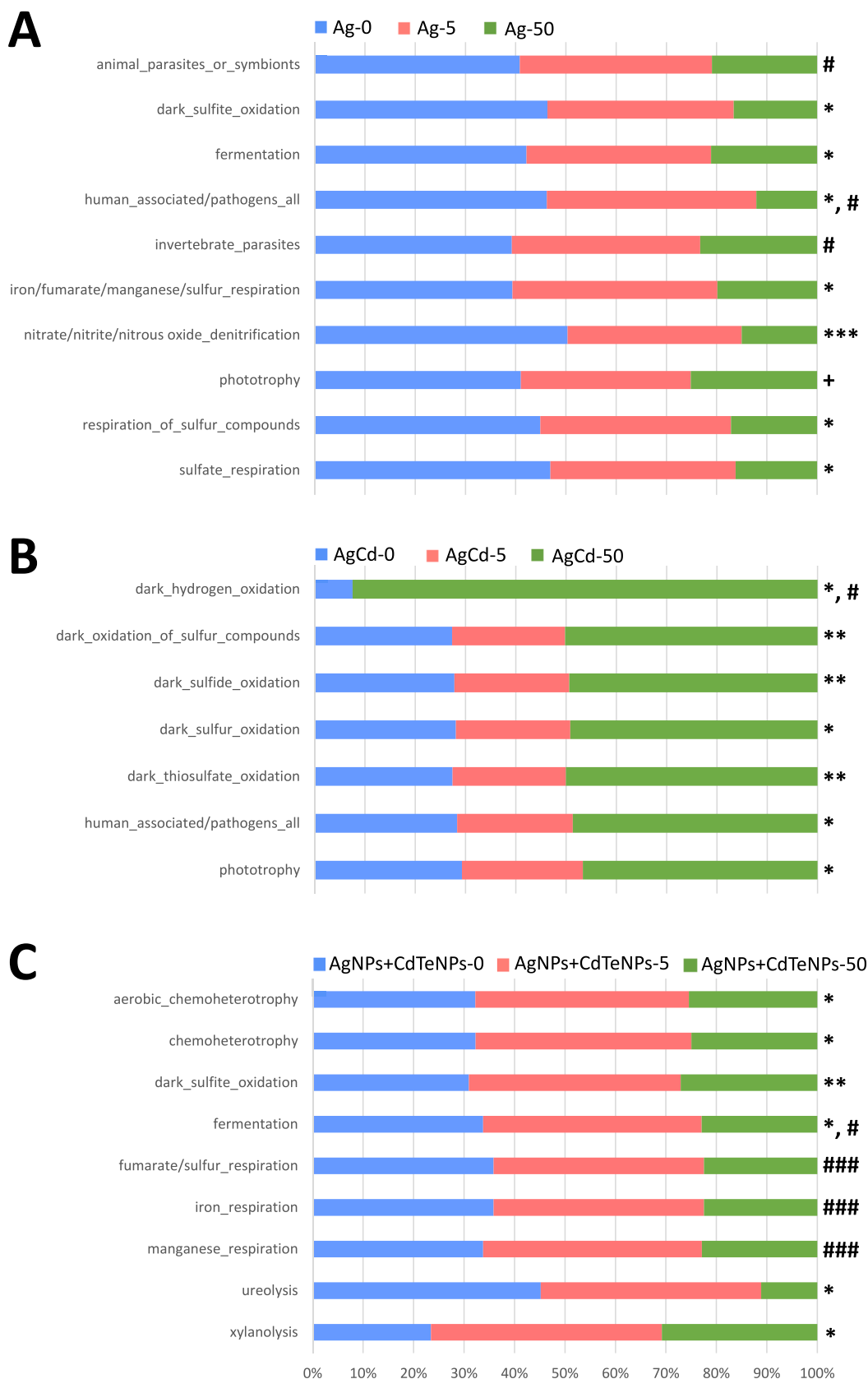
**Fig. 5.** FAPROTAX analysis of the functional changes that occur in the sediment when exposed to Ag and/or Cd in metallic or nanoparticle forms. Functions that presented significant changes after exposure to Ag (A), and to the mixtures Ag + Cd (B) and AgNPs+CdTeNPs (C) are represented. Similar functions have been grouped. Symbols on the right of the figure represent the significance: +, 5 *vs.* 0 μg L$^{-1}$; *, 50 *vs.* 0 μg L$^{-1}$; #, 50 *vs.* 5 μg L$^{-1}$. One symbol, $p < 0.05$; two symbols, $p < 0.01$; three symbols, $p < 0.001$.

As the vast majority of bacteria cells are unculturable, 16S rDNA sequencing has proven to be a powerful tool in the study of the bacteriome from complex abiotic matrixes (see following references).

### 4.3. Changes in the structure and functionality of the bacteriome in response to metals

Globally, the bacteriome described in this work is similar to those from other worldwide coastal and riverine sediments, with Proteobacteria, Bacteriodetes or Cyanobacteria as the common abundant phyla (Borsetto et al., 2021; Chen et al., 2022; Habibi et al., 2023; Mustafa et al., 2016; Qiu et al., 2020; Yin et al., 2022; Zhu et al., 2022). We did not detect any significant changes in the bacteriome of the sediments analyzed related to Ag and/or Cd exposures at this taxonomic level. Nevertheless, previous studies have observed that declines in: Nitrospirae, Actinobacteria, Verrumicrobia, Planctomycetesor Bacteriodetes phyla were related to other metal contents, such as Hg, Cr, Pb, Ni, or Zn (Li et al., 2020a; Qiu et al., 2020). However, these studies were performed by analyzing field samples and could have been affected by many other variables. Thus, the effects of Ag/Cd, both in their ionic or NP forms, were evaluated at the family taxon level.

A global PLS-DA showed that changes caused by exposure to Ag and/or Cd, both in their ionic or NP forms at the family level, could be used to differentiate unexposed sediments to those exposed to any of the metals clearly, even though the two doses used overlapped in their responses (Fig. 3), suggesting than even small amounts of the metals could cause alterations in the structure of the bacteriome of the sediments. Further, the α-diversity of the communities was compared between metal/s exposed and unexposed sediments to analyze the effects of the metals globally (Campo and Duval, 2014; Thukral, 2017). A decline in an ecosystems biodiversity is often related to negative consequences for its functions such as production, efficiency in using resources, and nutrient cycling (Xun et al., 2021). Surprisingly, although many families were significantly affected by the presence of Ag, Cd or Ag + Cd ions, the global α-biodiversity of the sediments did not change (Table S9), suggesting that alterations among bacterial families compensate each other and the global health of the bacteriome may not be impacted negatively. A recent report has associated the presence of similar levels of Cd with a decrease in the α-diversity of the bacterial community although the study was made in a natural polluted environment containing several metals and, thus, the interpretation of the results could be far more complex (Yu et al., 2023). On the other hand, even though one significant change was only found related to the presence of AgNPs+CdTeNPs, which was a decline in the Nocardiaceae family, the global α-biodiversity of the community seems to be significatively diminished at the highest dose used of the NP mixture (Fig. 2, Table S9). Nocardiaceae members are widely distributed in aquatic and terrestrial habitats and they are often related to the saprophytic digestion and recycling of organic material (Goodfellow, 2014). This family belongs to the Actinomycetes, characterized by their ability to decompose a wide range of substances, many of which are particularly important for the carbon cycle, *e.g.*, lignin, keratin or cellulose. Thus, a decrease in its abundance could be related to a decrease in the chemoheterotrophic capacity predicted for AgNPs+CdTeNPs contaminated sediments (Fig. 5). Furthermore, several other functionalities were significantly altered upon exposure to these NPs (Fig. 5), such as the fermentation and the anaerobic respiration of several compounds, suggesting that small changes in the abundance of certain families could accumulate and alter the ecosystem's equilibrium, thus considerably affecting its health.

Several bacterial families were affected by the presence of the Ag ions, most of them adversely, in agreement with the well-known bactericide effect of silver (Wakshlak et al., 2015; Xu et al., 2021). Both Ag ions and AgNPs are proven antibacterial agents. However, while the toxicity of ions has been related to interactions with the envelop of the bacterial cell, damage to biomolecules and the production of ROS, the antibacterial mode of AgNPs has not been well defined yet (Kędziora

et al., 2018). The Ag ions caused many more significant changes in the bacteriome of the sediments analyzed in this work than the corresponding nanoparticles. Seventeen families presented altered abundances, and all but two were negatively affected by Ag (Table 1, Fig. 4). This trend could be also observed in the predicted functionality of the microbiome, with several functions clearly diminished when exposed to Ag (Fig. 5). The reduction, when exposed to Ag, observed in the relative abundance of sequences from the bacterial families: Bacillaceae, Clostridiaceae, Erysipelotrichaceae, Moracellaceae or Spirochaetaceae reflects a decrease in the functions related to pathogens and parasites as several members of these families are well-known pathogens to humans and insects (Kaakoush, 2015; Karami et al., 2014; Mandic-Mulec et al., 2016; Teixeira and Merquior, 2014; Wiegel et al., 2006). Exposure to Ag was also associated with a decrease in several relevant metabolic functions related to the anaerobic respiration of inorganic ions such as iron, manganese, sulfate, sulfite, sulfur, nitrate, nitrite, *etc.* (Fig. 5), including a 10-fold decrease in the abundance of the Desulforomonadaceae family that can use a variety of compounds as electron acceptors and has an important role in carbon cycling and global warming (Greene, 2014; Katrin et al., 2012). For instance, the resulting biogeochemical metal cycles associated with dissimilatory iron and/or manganese reduction have a strong impact on many other elements including carbon, sulfur, phosphorous, and trace metals (Lovley et al., 2004; Nealson and Saffarini, 1994). Of ecological relevance is also the use of nitrate as a terminal electron acceptor, or dissimilatory denitrification, the main route by which fixed nitrogen is returned to the atmosphere as $N_2$ (Simon and Klotz, 2013).

Although Ag nanoparticles are widely used for their antibacterial properties, previous reports on their environmental toxicity showed contradictory results, depending on the experimental conditions, *e.g.*, concentration, exposure times, natural or artificial aquatic environments, presence of other pollutants, NP type, *etc.* (Jiang et al., 2017; Kusi et al., 2020; Yonathan et al., 2022). In our case, exposure to AgNPs was less toxic that to Ag, as it provoked little changes in the abundance of families and did not alter the α-diversity of the bacteriome, in concordance with most studies (Jiang et al., 2017; Yonathan et al., 2022).

Although a global cluster analysis of the families in the sediments when exposed to the Cd and Ag + Cd ions showed similar patterns, the taxons affected were not generally coincident (Fig. 4). Exposure to Cd, particularly at the highest dose used, caused an increase in several families such as: Alcanivoracaceae, Peptococcaceae, Thermoleophilaceae or unclassified Dehalococcoidia, that have been linked to several diverse functions including chemoheterotrophic metabolism. However, the FAPROTAX analysis did not predict any significant change in the global potential functionality of the bacteriome. On the other hand, exposure to the combination of Ag and Cd ions provoked the highest number of changes at the family level in the bacteriome of the sediments, with 24 families affected, 21 of which increased in abundance. Some of the increments were very prominent, with families such as Desulfuromonadaceae or Xanthobacteraceae being >20-fold more abundant in the sediments polluted by Ag + Cd. This could be related to the significant increase in functions related to chemoheterotrophy or the oxidation of hydrogen and sulfur compounds (Greene, 2014; Oren, 2014). Hydrogen-oxidizing bacteria are characterized by the use of hydrogen as an electron donor coupled with the ability to synthesize organic matter, through the reductive assimilation of $CO_2$ (Ananthararaman et al., 2013). The sulfur oxidizing microorganisms also play an important role in carbon sequestration (Hawley et al., 2014; Mattes et al., 2013). Additionally, these microorganisms provide carbon to motile eukaryotic organisms (*e.g.*, bivalves, nematodes, flatworms, ciliates, *etc.*) through a symbiotic relationship in which the host provides access to reduced sulfur sources (Dubilier et al., 2008; Mattes et al., 2013). Also, a considerable increase in bacterial families that include pathogens such as Bacillaceae, Piscirickettsiaceae or Spirochaetaceae could be observed in the presence of the metals. Taken together, these results suggest that the effects on the sediment microbiome of exposure

to Ag and Cd are not merely summary as their interaction may cause a more complex response.

Finally, although AgNPs+CdTeNPs only caused significant changes in the abundance of the Nocardiaceae family, essential functionalities were significantly altered when exposed to these NPs, suggesting that small changes could add up and alter the biogeochemical cycles in the sediments. In this regard, it is worth noting the very significant decrease in the anaerobic respiration of different compounds (iron, manganese, fumarate and sulfur), which occurred after exposure to Ag.

## 5. Conclusion

This study explored changes in the abundance, composition, and diversity of the bacterial communities from sediments within a microcosm exposed to silver and cadmium, either individually or as a mixture, in both their ionic and NP forms. Specifically, our results provided evidence that: (1) AgNPs and/or CdTeNPs caused less significant family-specific shifts in the sediment bacteriome than their corresponding ionic forms; (2) nevertheless, the global α-biodiversity of the bacteriome was reduced only when exposed to the AgNPs+CdTeNPs mixture, suggesting that pivotal functional processes maybe compromised; (3) Ag provoked a significant decrease in the abundance of several bacterial families, and the potential functionalities associated to this bacteriome, while Cd or the Ag + Cd mixture caused general increments in both parameters; and (4) although AgNPs+CdTeNPs only significantly affected the abundance of the Nocardiaceae family, the diversity and the potential functionality of the sediments were compromised. When approaches such as these ones are applied to environmental problems, they may help us to understand the feedback mechanism of microorganisms' response to stressful changes in the aquatic/terrestrial environment better, and thereby elucidate how their global functional processes can be modified.

Supplementary data to this article can be found online at https://doi.org/10.1016/j.marpolbul.2024.116525.

## CRediT authorship contribution statement

**Ana M. Herruzo-Ruiz:** Writing – original draft, Methodology, Investigation, Formal analysis, Conceptualization. **Chiara Trombini:** Writing – original draft, Methodology, Investigation, Formal analysis, Conceptualization. **Ignacio Moreno-Garrido:** Conceptualization, Formal analysis, Investigation, Methodology, Writing – review & editing. **Julián Blasco:** Writing – review & editing, Writing – original draft, Supervision, Resources, Project administration, Methodology, Investigation, Funding acquisition, Conceptualization. **José Alhama:** Writing – review & editing, Writing – original draft, Visualization, Resources, Project administration, Methodology, Investigation, Funding acquisition, Conceptualization. **Carmen Michán:** Writing – review & editing, Writing – original draft, Supervision, Resources, Project administration, Methodology, Investigation, Funding acquisition, Conceptualization.

## Declaration of Generative AI and AI-assisted technologies in the writing process

The authors have not employed AI or AI-assisted technologies for writing this manuscript.

## Declaration of competing interest

The authors declare that they have no known competing financial interests or personal relationships that could have appeared to influence the work reported in this paper.

## Data availability

Data will be made available on request.

## References

Abu Bakar, N.F., Tan, H.L., Lim, Y.P., Adrus, N., Abdullah, J., 2022. Environmental impact of quantum dots. In: Graphene, Nanotubes and Quantum Dots-Based Nanotechnology Fundamentals and Applications, pp. 837–867. https://doi.org/10.1016/b978-0-323-85457-3.00011-6.

Algül, F., Beyhan, M., 2020. Concentrations and sources of heavy metals in shallow sediments in Lake Bafa. Turkey. Sci. Rep. 10, 1–12. https://doi.org/10.1038/s41598-020-68833-2.

Ali, H., Khan, E., Ilahi, I., 2019. Environmental chemistry and ecotoxicology of hazardous heavy metals: environmental persistence, toxicity, and bioaccumulation. J. Chem. 2019, 6730305. https://doi.org/10.1155/2019/6730305.

Amat, F., Hontoria, F., Ruiz, O., Green, A.J., Sánchez, M.I., Figuerola, J., Hortas, F., 2005. The American brine shrimp as an exotic invasive species in the western Mediterranean. Biol. Invasions 7, 37–47. https://doi.org/10.1007/s10530-004-9634-9.

Anantharaman, K., Breier, J.A., Sheik, C.S., Dick, G.J., 2013. Evidence for hydrogen oxidation and metabolic plasticity in widespread deep-sea sulfur-oxidizing bacteria. Proc. Natl. Acad. Sci. 110, 330–335. https://doi.org/10.1073/pnas.1215340110.

Averill, C., Anthony, M.A., Baldrian, P., Finkbeiner, F., Hoogen, J., Van Den Kiers, T., Kohout, P., Hirt, E., Smith, G.R., Crowther, T.W., 2022. Defending Earth's terrestrial microbiome. Nat. Microbiol. 7, 1717–1725. https://doi.org/10.1038/s41564-022-01228-3.

Babaei, M., Tayemeh, M.B., Jo, M.S., Yu, I.J., Johari, S.A., 2022. Trophic transfer and toxicity of silver nanoparticles along a phytoplankton-zooplankton-fish food chain. Sci. Total Environ. 842, 156807 https://doi.org/10.1016/j.scitotenv.2022.156807.

Bejaoui, S., Michán, C., Telahigue, K., Nechi, S., el Cafsi, M., Soudani, N., Blasco, J., Costa, P.M., Alhama, J., 2020. Metal body burden and tissue oxidative status in the bivalve *Venerupis decussata* from Tunisian coastal lagoons. Mar. Environ. Res. 159, 105000 https://doi.org/10.1016/j.marenvres.2020.105000.

Bhuvaneshwari, M., Thiagarajan, V., Nemade, P., Chandrasekaran, N., Mukherjee, A., 2018. Toxicity and trophic transfer of P25 TiO2 NPs from *Dunaliella salina* to *Artemia salina*: effect of dietary and waterborne exposure. Environ. Res. 160, 39–46. https://doi.org/10.1016/j.envres.2017.09.022.

Borsetto, C., Raguideau, S., Travis, E., Kim, D.W., Lee, D.H., Bottrill, A., Stark, R., Song, L., Cha, C.J., Pearson, J., Quince, C., Singer, A.C., Wellington, E.M.H., 2021. Impact of sulfamethoxazole on a riverine microbiome. Water Res. 201, 117382 https://doi.org/10.1016/j.watres.2021.117382.

Bowler, C., Allen, A., Badger, J., et al., 2008. The Phaeodactylum genome reveals the evolutionary history of diatom genomes. Nature 456, 239–244. https://doi.org/10.1038/nature07410.

Campo, A.M., Duval, V.S., 2014. Diversidad y valor de importancia para la conservación de la vegetación natural. Parque Nacional Lihué Calel (Argentina). An. Geogr. la Univ. Complut. 34, 25–42. https://doi.org/10.5209/rev_AGUC.2014.v34.n2.47071.

Celis-Hernández, O., Ontiveros-Cuadras, J.F., Ward, R.D., Girón-García, M.P., Pérez-Ceballos, R.Y., Canales-Delgadillo, J.C., Acevedo-Granados, I.V., Santiago-Pérez, S., Armstrong-Altrin, J.S., Merino-Ibarra, M., 2022. Biogeochemical behaviour of cadmium in sediments and potential biological impact on mangroves under anthropogenic influence: a baseline survey from a protected nature reserve. Mar. Pollut. Bull. 185, 114260 https://doi.org/10.1016/j.marpolbul.2022.114260.

Chen, C., Pan, J., Xiao, S., Wang, J., Gong, X., Yin, G., Hou, L., Liu, M., Zheng, Y., 2022. Microplastics alter nitrous oxide production and pathways through affecting microbiome in estuarine sediments. Water Res. 221, 118733 https://doi.org/10.1016/j.watres.2022.118733.

Chronakis, M.I., Mavrakis, E., Garcia, R.A., et al., 2023. Investigating the behavior of ultratrace levels of nanoparticulate and ionic silver in a seawater mesocosm using single particle inductively coupled plasma - mass spectrometry. Chemosphere 336, 139109. https://doi.org/10.1016/j.chemosphere.2023.139109.

Dubilier, N., Bergin, C., Lott, C., 2008. Symbiotic diversity in marine animals: the art of harnessing chemosynthesis. Nat. Rev. Microbiol. 6, 725–740. https://doi.org/10.1038/nrmicro1992.

El-Rayis, O.A., 1985. Re-assessment of the titration method for determination of organic carbon in recent sediments. Rapports et procès-verbaux des réunions Commission Interantionale pour l'Exploration Scientifique de la Mer Méditerranée 29, 45–47.

Freitas, R., Almeida, Â., Calisto, V., Velez, C., Moreira, A., Schneider, R.J., Esteves, V.I., Wrona, F.J., Figueira, E., Soares, A.M.V.M., 2016. The impacts of pharmaceutical drugs under ocean acidification: new data on single and combined long-term effects of carbamazepine on *Scrobicularia plana*. Sci. Total Environ. 541, 977–985. https://doi.org/10.1016/j.scitotenv.2015.09.138.

Gaudette, H.E., Flight, W.R., Toner, L., Folger, D., 1974. An inexpensive titration method of organic carbon in recent sediments. J. Sediment. Petrol. 44, 249–253. https://doi.org/10.1306/74d729d7-2b21-11d7-8648000102c1865d.

Giese, B., Klaessig, F., Park, B., Kaegi, R., Steinfeldt, M., Wigger, H., von Gleich, A., Gottschalk, F., 2018. Risks, release and concentrations of engineered nanomaterial in the environment. Sci. Rep. 8, 1–18. https://doi.org/10.1038/s41598-018-19275-4.

Goodfellow, M., 2014. The family Nocardiaceae. In: Rosenberg, E., DeLong, E.F., Lory, S., Stackebrandt, E., Thompson, F. (Eds.), The Prokaryotes: Actinobacteria. Springer, Berlin Heidelberg, Berlin, Heidelberg, pp. 595–650. https://doi.org/10.1007/978-3-642-30138-4_404.

Graves, J.L., 2022. Multidrug-resistant microbes and the "magic bullet"—metallic, metallic oxides—nanoparticles. Principles and Aplications of Antimicrobial Nanomaterials Micro and Nano Technologies 63-83. https://doi.org/10.1016/B978-0-12-822105-1.00005-6.

Greene, A.C., 2014. In: Rosenberg, E., DeLong, E.F., Lory, S., Stackebrandt, E., Thompson, F. (Eds.), The Family Desulfuromonadaceae BT- The Prokaryotes: Deltaproteobacteria and Epsilonproteobacteria. Springer Berlin Heidelberg, Berlin, Heidelberg, pp. 143–155. https://doi.org/10.1007/978-3-642-39044-9_380.

Habibi, N., Uddin, S., Al-Sarawi, H., Aldhameer, A., Shajan, A., Zakir, F., Abdul Razzack, N., Alam, F., 2023. Metagenomes from coastal sediments of Kuwait: insights into the microbiome. Metabolic Functions and Resistome. Microorganisms 11, 531. https://doi.org/10.3390/microorganisms11020531.

Hawley, A.K., Brewer, H.M., Norbeck, A.D., Paša-Tolić, L., Hallam, S.J., 2014. Metaproteomics reveals differential modes of metabolic coupling among ubiquitous oxygen minimum zone microbes. Proc. Natl. Acad. Sci. 111, 11395–11400. https://doi.org/10.1073/pnas.1322132111.

Hu, X., Wang, J., Lv, Y., Liu, X., Zhong, J., Cui, X., Zhang, M., Ma, D., Yan, X., Zhu, X., 2021. Effects of heavy metals/metalloids and soil properties on microbial communities in farmland in the vicinity of a metals smelter. Front. Microbiol. 12, 1–13. https://doi.org/10.3389/fmicb.2021.707786.

Jiang, H.S., Yin, L., Ren, N.N., Xian, L., Zhao, S., Li, W., Gontero, B., 2017. The effect of chronic silver nanoparticles on aquatic system in microcosms. Environ. Pollut. 223, 395–402. https://doi.org/10.1016/j.envpol.2017.01.036.

Kaakoush, N.O., 2015. Insights into the role of Erysipelotrichaceae in the human host. Front. Cell. Infect. Microbiol. 5, 1–4. https://doi.org/10.3389/fcimb.2015.00084.

Kalman, J., Smith, B.D., Bury, N.R., Rainbow, P.S., 2014. Biodynamic modelling of the bioaccumulation of trace metals (Ag, As and Zn) by an infaunal estuarine invertebrate, the clam *Scrobicularia plana*. Aquat. Toxicol. 154, 121–130. https://doi.org/10.1016/j.aquatox.2014.05.011.

Karami, A., Sarshar, M., Ranjbar, R., Zanjani, R.S., 2014. In: Rosenberg, E., DeLong, E.F., Lory, S., Stackebrandt, E., Thompson, F. (Eds.), The Phylum Spirochaetaceae BT - the Prokaryotes: Other Major Lineages of Bacteria and the Archaea. Springer, Berlin Heidelberg, Berlin, Heidelberg, pp. 915–929. https://doi.org/10.1007/978-3-642-38954-2_156.

Katrin, R., Marcus, S., Johannes, G., 2012. Dissimilatory reduction of extracellular electron acceptors in anaerobic respiration. Appl. Environ. Microbiol. 78, 913–921. https://doi.org/10.1128/AEM.06803-11.

Kędziora, A., Speruda, M., Krzyżewska, E., Rybka, J., Łukowiak, A., Bugla-Płoskońska, G., 2018. Similarities and differences between silver ions and silver in nanoforms as antibacterial agents. Int. J. Mol. Sci. 19, 444. https://doi.org/10.3390/ijms19020444.

Kennish, M.J., 2000. Practical Handbook of Marine Science. CRC Press, Boca Raton, Florida, p. 896.

Krom, M.D., 1980. Spectrophotometric a study of a determination of ammonia: modified Berthelot reaction using salicylate and dichloroisocyanurate. Analyst 105 (1249), 305–316.

Kusi, J., Scheuerman, P.R., Maier, K.J., 2020. Emerging environmental contaminants (silver nanoparticles) altered the catabolic capability and metabolic fingerprinting of microbial communities. Aquat. Toxicol. 228, 105633 https://doi.org/10.1016/j.aquatox.2020.105633.

Levy, J.L., Angel, B.M., Staubera, J.L., Poonc, W.L., Simpson, S.L., Cheng, S.J., Jolley, D. F., 2008. Uptake and internalisation of copper by three maroine microalgae. Comparison of copper-sensitive and copper tolerant species. Aquat. Toxicol. 89, 82–93. https://doi.org/10.1016/j.aquatox.2008.06.003.

Li, C., Quan, Q., Gan, Y., Dong, J., Fang, J., Wang, L., Liu, J., 2020a. Effects of heavy metals on microbial communities in sediments and establishment of bioindicators based on microbial taxa and function for environmental monitoring and management. Sci. Total Environ. 749, 141555 https://doi.org/10.1016/j.scitotenv.2020.141555.

Li, P., Su, M., Wang, X., et al., 2020b. Environmental fate and behavior of silver nanoparticles in natural estuarine systems. J. Environ. Sci. (China) 88, 248–259. https://doi.org/10.1016/j.jes.2019.09.013.

Locey, K.J., Lennon, J.T., 2016. Scaling laws predict global microbial diversity. Proc. Natl. Acad. Sci. U. S. A. 113, 5970–5975. https://doi.org/10.1073/pnas.1521291113.

Louca, S., Parfrey, L.W., Doebeli, M., 2016. Decoupling function and taxonomy in the global ocean microbiome. Science 16 (353), 1272–1277.

Lovley, D.R., Holmes, D.E., Nevin, K.P.B.T.-A. in M.P., 2004. Dissimilatory Fe(III) and Mn (IV) Reduction. Academic Press, pp. 219–286. https://doi.org/10.1016/S0065-2911(04)49005-5.

Mandic-Mulec, I., Stefanic, P., van Elsas, J.D., 2016. Ecology of bacillaceae. Bact. Spore From Mol. to Syst. 59–85 https://doi.org/10.1128/9781555819323.ch3.

Mattes, T.E., Nunn, B.L., Marshall, K.T., Proskurowski, G., Kelley, D.S., Kawka, O.E., Goodlett, D.R., Hansell, D.A., Morris, R.M., 2013. Sulfur oxidizers dominate carbon fixation at a biogeochemical hot spot in the dark ocean. ISME J. 7, 2349–2360. https://doi.org/10.1038/ismej.2013.113.

Metcalfe, C.D., Sultana, T., Martin, J., Newman, K., Helm, P., Kleywegt, S., Shen, L., Yargeau, V., 2018. Silver near municipal wastewater discharges into western Lake Ontario. Canada. Environ. Monit. Assess. 190, 555. https://doi.org/10.1007/s10661-018-6922-x.

Mouneyrac, C., Buffet, P.E., Poirier, L., et al., 2014. Fate and effects of metal-based nanoparticles in two marine invertebrates, the bivalve mollusc *Scrobicularia plana* and the annelid polychaete *Hediste diversicolor*. Environ. Sci. Pollut. Res. Int. 21, 7899–7912. https://doi.org/10.1007/s11356-014-2745-7.

Mustafa, G.A., Abd-Elgawad, A., Ouf, A., Siam, R., 2016. The Egyptian Red Sea coastal microbiome: a study revealing differential microbial responses to diverse anthropogenic pollutants. Environ. Pollut. 214, 892–902. https://doi.org/10.1016/j.envpol.2016.04.009.

Ndungu, K., 2011. Dissolved silver in the Baltic Sea. Environ. Res. 111, 45–49. https://doi.org/10.1016/j.envres.2010.09.015.

Nealson, K.H., Saffarini, D., 1994. Iron and manganese in anaerobic respiration: environmental significance, physiology, and regulation. Annu. Rev. Microbiol. 48, 311–343. https://doi.org/10.1146/annurev.mi.48.100194.001523.

Oh, E., Liu, R., Nel, A., Gemill, K.B., Bilal, M., Cohen, Y., Medintz, I.L., 2016. Meta-analysis of cellular toxicity for cadmium-containing quantum dots. Nat. Nanotechnol. 11, 479–486. https://doi.org/10.1038/nnano.2015.338.

Oren, A., 2014. In: Rosenberg, E., DeLong, E.F., Lory, S., Stackebrandt, E., Thompson, F. (Eds.), The Family Xanthobacteraceae BT - The Prokaryotes: Alphaproteobacteria and Betaproteobacteria. Springer Berlin Heidelberg, Berlin, Heidelberg, pp. 709–726. https://doi.org/10.1007/978-3-642-30197-1_258.

Pan, F., Wang, B., Zhang, Y., et al., 2022. Bioavailability, (im)mobilization kinetics, and spatiotemporal patterns of arsenic and cadmium in surficial sediments of a river–estuary–coast system. J. Hydrol. 612, 128140 https://doi.org/10.1016/j.jhydrol.2022.128140.

Qiu, H., Gu, L., Sun, B., Zhang, J., Zhang, M., He, S., An, S., Leng, X., 2020. Metagenomic analysis revealed that the terrestrial pollutants override the effects of seasonal variation on microbiome in river sediments. Bull. Environ. Contam. Toxicol. 105, 892–898. https://doi.org/10.1007/s00128-020-03033-2.

Reul, A., Muñoz, M., Criado-Aldeanueva, F., Rodríguez, V., 2006. Spatial distribution of phytoplankton > 13μm in the gulf of Cádiz in relation to water masses and circulation pattern under westerly and easterly wind regimes. Deep-Sea Research II 53, 1294–1313.

Rocha, T.L., Gomes, T., Sousa, V.S., Mestre, N.C., Bebianno, M.J., 2015a. Ecotoxicological impact of engineered nanomaterials in bivalve molluscs: an overview. Mar. Environ. Res. 111, 74–88. https://doi.org/10.1016/j.marenvres.2015.06.013.

Rocha, T.L., Gomes, T., Pinheiro, J.P., et al., 2015b. Toxicokinetics and tissue distribution of cadmium-based quantum dots in the marine mussel *Mytilus galloprovincialis*. Environ. Pollut. 204, 207–214. https://doi.org/10.1016/j.envpol.2015.05.008.

Rzigalinski, B.A., Strobl, J.S., 2009. Cadmium-containing nanoparticles: perspectives on pharmacology and toxicology of quantum dots. Toxicol. Appl. Pharmacol. 238, 280–288. https://doi.org/10.1016/j.taap.2009.04.010.

Sall, M.L., Diaw, A.K.D., Gningue-Sall, D., Efremova Aaron, S., Aaron, J.J., 2020. Toxic heavy metals: impact on the environment and human health, and treatment with conducting organic polymers, a review. Environ. Sci. Pollut. Res. Int. 27, 29927–29942. https://doi.org/10.1007/s11356-020-09354-3.

Sendra, M., Yeste, M.P., Gatica, J.M., Moreno-Garrido, I., Blasco, J., 2017. Direct and indirect effects of silver nanoparticles on freshwater and marine microalgae (*Chlamydomonas reinhardtii* and *Phaeodactylum tricornutum*). Chemosphere 179, 279–289. https://doi.org/10.1016/j.chemosphere.2017.03.123.

Serafim, A., Bebianno, M.J., 2010. Effect of a polymetallic mixture on metal accumulation and metallothionein response in the clam *Ruditapes decussatus*. Aquat. Toxicol. 99, 370–378. https://doi.org/10.1016/j.aquatox.2010.05.016.

Simon, J., Klotz, M.G., 2013. Diversity and evolution of bioenergetic systems involved in microbial nitrogen compound transformations. Biochim. Biophys. Acta Bioenerg. 1827, 114–135. https://doi.org/10.1016/j.bbabio.2012.07.005.

Solanki, R.G., Rajaram, P., 2017. Structural, optical and morphological properties of CdS nanoparticles synthesized using hydrazine hydrate as a complexing agent. Nano-Structures and Nano-Objects 12, 157–165. https://doi.org/10.1016/j.nanoso.2017.10.003.

Solé, M., Kopecka-Pilarczyk, J., Blasco, J., 2009. Pollution biomarkers in two estuarine invertebrates, *Nereis diversicolor* and *Scrobicularia plana*, from a Marsh ecosystem in SW Spain. Environ. Int. 35, 523–531. https://doi.org/10.1016/j.envint.2008.09.013.

Sturn, A., Quackenbush, J., Trajanoski, Z., 2002. Genesis: cluster analysis of microarray data. Bioinformatics 18, 207–208. https://doi.org/10.1093/bioinformatics/18.1.207.

Tang, W., Shan, B., Zhang, W., Zhang, H., Wang, L., Ding, Y., 2014. Heavy metal pollution characteristics of surface sediments in different aquatic ecosystems in eastern China: a comprehensive understanding. PloS One 9. https://doi.org/10.1371/journal.pone.0108996.

Tao, W., Chen, G., Zeng, G., Yan, M., Chen, A., Guo, Z., Huang, Z., He, K., Hu, L., Wang, L., 2016. Influence of silver nanoparticles on heavy metals of pore water in contaminated river sediments. Chemosphere 162, 117–124. https://doi.org/10.1016/j.chemosphere.2016.07.043.

Teixeira, L.M., Merquior, V.L.C., 2014. In: Rosenberg, E., DeLong, E.F., Lory, S., Stackebrandt, E., Thompson, F. (Eds.), The Family Moraxellaceae BT- The Prokaryotes: Gammaproteobacteria. Springer Berlin Heidelberg, Berlin, Heidelberg, pp. 443–476. https://doi.org/10.1007/978-3-642-38922-1_245.

Thukral, A.K., 2017. A review on measurement of alpha diversity in biology. Agric. Res. J. 54, 1. https://doi.org/10.5958/2395-146x.2017.00001.1.

Tian, X., Xu, W., Wang, F., Ye, Y., Liu, M., Shi, H., Fan, D., Xu, F., 2022. Heavy metals in the sediments of Laoshan Bay, China: distribution and contamination assessment. Mar. Pollut. Bull. 185, 114264 https://doi.org/10.1016/j.marpolbul.2022.114264.

Vanni, I., Coco, S., Truini, A., Rusmini, M., Dal Bello, M.G., Alama, A., Banelli, B., Mora, M., Rijavec, E., Barletta, G., Genova, C., Biello, F., Maggioni, C., Grossi, F., 2015. Next-generation sequencing workflow for NSCLC critical samples using a targeted sequencing approach by ion torrent PGMTM platform. Int. J. Mol. Sci. 16, 28765–28782. https://doi.org/10.3390/ijms161226129.

Volland, M., Hampel, M., Martos-Sitcha, J.A., Trombini, C., Martínez-Rodríguez, G., Blasco, J., 2015. Citrate gold nanoparticle exposure in the marine bivalve *Ruditapes philippinarum*: uptake, elimination and oxidative stress response. Environ. Sci. Pollut. Res. 22, 17414–17424. https://doi.org/10.1007/s11356-015-4718-x.

Wakshlak, R.B.K., Pedahzur, R., Avnir, D., 2015. Antibacterial activity of silver-killed bacteria: the "zombies" effect. Sci. Rep. 5, 1–5. https://doi.org/10.1038/srep09555.

Wang, Y., Bao, G., 2022. Diversity of prokaryotic microorganisms in alkaline saline soil of the Qarhan Salt Lake area in the Qinghai–Tibet Plateau. Sci. Rep. 12, 1–14. https://doi.org/10.1038/s41598-022-07311-3.

Wang, L., Li, Y., Zhao, Z., Cordier, T., Worms, I.A., Niu, L., Fan, C., Slaveykova, V.I., 2021. Microbial community diversity and composition in river sediments contaminated with tetrabromobisphenol A and copper. Chemosphere 272. https://doi.org/10.1016/j.chemosphere.2021.129855.

Wiegel, J., Tanner, R., Rainey, F.A., 2006. In: Dworkin, M., Falkow, S., Rosenberg, E., Schleifer, K.-H., Stackebrandt, E (Eds.), An Introduction to the Family Clostridiaceae BT - The Prokaryotes: Volume 4: Bacteria: Firmicutes, Cyanobacteria. Springer US, New York, NY, pp. 654–678. https://doi.org/10.1007/0-387-30744-3_20.

Wimmer, A., Urstoeger, A., Funck, N.C., et al., 2020. What happens to silver-based nanoparticles if they meet seawater? Water Res. 171, 115399 https://doi.org/10.1016/j.watres.2019.115399.

Xu, Z., Zhang, C., Wang, X., Liu, D., 2021. Release strategies of silver ions from materials for bacterial killing. ACS Appl. Bio Mater. 4, 3985–3999. https://doi.org/10.1021/acsabm.0c01485.

Xun, W., Liu, Y., Li, W., Ren, Y., Xiong, W., Xu, Z., Zhang, N., Miao, Y., Shen, Q., Zhang, R., 2021. Specialized metabolic functions of keystone taxa sustain soil microbiome stability. Microbiome 9, 1–15. https://doi.org/10.1186/s40168-020-00985-9.

Yang, Z., Peng, C., Cao, H., Song, J., Gong, B., Li, L., Wang, L., He, Y., Liang, M., Lin, J., Lu, L., 2022. Microbial functional assemblages predicted by the FAPROTAX analysis are impacted by physicochemical properties, but C, N and S cycling genes are not in mangrove soil in the Beibu Gulf. China. Ecol. Indic. 139, 108887 https://doi.org/10.1016/j.ecolind.2022.108887.

Yin, X., Wang, W., Wang, A., He, M., Lin, C., Ouyang, W., Liu, X., 2022. Microbial community structure and metabolic potential in the coastal sediments around the Yellow River Estuary. Sci. Total Environ. 816, 151582 https://doi.org/10.1016/j.scitotenv.2021.151582.

Yonathan, K., Mann, R., Mahbub, K.R., Gunawan, C., 2022. The impact of silver nanoparticles on microbial communities and antibiotic resistance determinants in the environment. Environ. Pollut. 293, 118506 https://doi.org/10.1016/j.envpol.2021.118506.

Yu, C., Zhu, Z., Meng, K., Zhang, H., Xu, M., 2023. Unveiling the impact and mechanisms of Cd-driven ecological assembly and coexistence of bacterial communities in coastal sediments of Yellow Sea. J. Hazard. Mater. 460, 132309 https://doi.org/10.1016/j.jhazmat.2023.132309.

Yuan, L., Richardson, C.J., Ho, M., Willis, C.W., Colman, B.P., Wiesner, M.R., 2018. Stress responses of aquatic plants to silver nanoparticles. Environ. Sci. Technol. 52, 2558–2565. https://doi.org/10.1021/acs.est.7b05837.

Zhang, H., Reynolds, M., 2019. Cadmium exposure in living organisms: a short review. Sci. Total Environ. 678, 761–767. https://doi.org/10.1016/j.scitotenv.2019.04.395.

Zhao, S., Feng, C., Wang, D., Liu, Y., Shen, Z., 2013. Salinity increases the mobility of Cd, Cu, Mn, and Pb in the sediments of Yangtze Estuary: relative role of sediments' properties and metal speciation. Chemosphere 91, 977–984. https://doi.org/10.1016/j.chemosphere.2013.02.001.

Zhao, J., Wang, X., Hoang, S.A., et al., 2021. Silver nanoparticles in aquatic sediments: occurrence, chemical transformations, toxicity, and analytical methods. J. Hazard. Mater. 418, 126368 https://doi.org/10.1016/j.jhazmat.2021.126368.

Zhu, L., Li, R., Yan, Y., Cui, L., 2022. Urbanization drives the succession of antibiotic resistome and microbiome in a river watershed. Chemosphere 301, 134707. https://doi.org/10.1016/j.chemosphere.2022.134707.